

1 Activation of the Dopaminergic Pathway from VTA to the Medial Olfactory Tubercle Generates
2 Odor-Preference and Reward

3

4 Zhijian Zhang^{1,2*}, Qing Liu^{1*}, Pengjie Wen¹, Jiaozhen Zhang¹, Xiaoping Rao¹, Ziming Zhou³, Hongruo
5 Zhang³, Xiaobin He¹, Juan Li¹, Zheng Zhou⁴, Xiaoran Xu³, Xueyi Zhang³, Rui Luo³, Guanghui Lv²,
6 Haohong Li², Pei Cao¹, Liping Wang⁴, Fuqiang Xu^{1,2}

7

8 ¹Center for Brain Science, Key Laboratory of Magnetic Resonance in Biological Systems and State Key
9 Laboratory of Magnetic Resonance and Atomic and Molecular Physics, Wuhan Institute of Physics and
10 Mathematics, CAS Center for Excellence in Brain Science and Intelligence Technology, Chinese Academy
11 of Sciences, Wuhan 430071, China; ²Wuhan National Laboratory for Optoelectronics, Wuhan 430074;
12 ³College of Life Sciences, Wuhan University, Wuhan 430072, China; ⁴Shenzhen Key Lab of
13 Neuropsychiatric Modulation and Collaborative Innovation Center for Brain Science, CAS Center for
14 Excellence in Brain Science, Shenzhen Institutes of Advanced Technology, Chinese Academy of Sciences,
15 Shenzhen 518055, China.

16

17 Address correspondence to Fuqiang Xu, Wuhan Institute of Physics and Mathematics, Chinese Academy of
18 Sciences, Xiao Hong-Shan, Wuhan, 430071, PR China; Email: fuqiang.xu@wipm.ac.cn, Tel:
19 +86-27-8719-7091, Fax: +86-27-8719-9543.

20 *authors with equal contribution to this work.

1 **Abstract**

2 Odor-preferences are usually influenced by life experiences. However, the neural circuit mechanisms remain
3 unclear. The medial olfactory tubercle (mOT) is involved in both reward and olfaction, while the ventral
4 tegmental area (VTA) dopaminergic (DAergic) neurons are considered to be engaged in reward and
5 motivation. Here, we found that the VTA (DAergic)-mOT pathway could be activated by different types of
6 naturalistic rewards as well as odors in DAT-cre mice. Optogenetic activation of the VTA-mOT DAergic
7 fibers was able to elicit preferences for space, location and neutral odor, while pharmacological blockade of
8 the dopamine receptors in the mOT fully prevented the odor-preference formation. Furthermore, inactivation
9 of the mOT-projecting VTA DAergic neurons eliminated the previously formed odor-preference and strongly
10 affected the Go-no go learning efficiency. In summary, our results revealed that the VTA (DAergic)-mOT
11 pathway mediates a variety of naturalistic reward processes and different types of preferences including
12 odor-preference in mice.

13 **Key words:** medial olfactory tubercle, odor-preference, reward, ventral tegmental area

15 **Introduction**

16 Sensory perceptions are influenced by life experiences. For us, it's a pleasure to unexpectedly smell the odor
17 of grandmother's cookies that we loved in our childhood, and people of different cultures may have different
18 odor-preferences, such as blue cheese to European and stinky bean-curd to Chinese. For rodents,
19 reward-related odor perception is critical for food foraging and reproduction (Doty 1986). The formation of
20 odor-preference should involve the interaction between the olfactory and reward systems, although the
21 mechanisms, the engaged brain regions and neural circuits are still unclear.

22 The olfactory tubercle (OT) is a long and narrow tubular brain structure located at the ventral part of
23 striatum. It belongs to the olfactory system and receives dense direct inputs from the main olfactory bulb
24 (OB) and other olfactory cortexes such as the anterior olfactory nucleus (AON) and piriform cortex (PCX)
25 (Wesson and Wilson 2011). As a part of the ventral striatum reward circuitry, the OT is also heavily
26 innervated by dopaminergic (DAergic) neurons from the ventral tegmental area (VTA, (Voorn et al. 1986)).

1 Belonging to both the olfactory and reward circuits (Ikemoto 2007, Wesson and Wilson 2011), the OT is at
2 the proper position to play critical roles in the formation of odor-preference. Previous results from relatively
3 limited studies are in agreement with this intuition. The OT encodes natural reinforcers (Gadziola and
4 Wesson 2016), odor valence and pheromone reward (Gadziola and Wesson 2016, DiBenedictis et al. 2015,
5 Agustin-Pavon, Martinez-Garcia, and Lanuza 2014), and also influences reward behaviors and
6 odor-preferences (FitzGerald, Richardson, and Wesson 2014). Furthermore, specific domains of the OT
7 represent reward or punishment associated odor-cues (Murata et al. 2015). These works have revealed that
8 the OT is involved in the formation of odor-preference. The OT directly receives olfactory inputs, however,
9 how it is regulated by the reward system to form odor-preferences, and whether it plays roles in other reward
10 behaviors are still largely unknown.

11 An earlier study showed that the VTA can modulate the activities of olfactory-related OT neurons
12 (Mooney et al. 1987). The VTA DAergic neurons have been proposed to play central roles in general reward
13 and motivation, *via* innervating the ventral striatum (Hu 2016, Roeper 2013, Ungless, Argilli, and Bonci
14 2010). As a component of the ventral striatum, most of the OT neurons are D1 and D2 dopamine
15 receptor-expressing medium spiny neurons (Murata et al. 2015, Millhouse and Heimer 1984), which are
16 heavily innervated by DAergic neurons from the VTA (Voorn et al. 1986). From these anatomical and
17 functional facts about the two brain regions, we hypothesized that the VTA (DAergic)-OT pathway play
18 pivotal roles in the formation of odor-preference and reward behaviors involving other modalities.
19 Compared with the lateral OT, the medial OT (mOT) is more involved in addiction, reward and reward
20 associated odor perceptions (Murata et al. 2015, Ikemoto 2005, 2003). In fact, the mOT mediates
21 self-administration of cocaine or D-amphetamine even more robustly than the nucleus accumbens (NAc),
22 which is crucially important for reward learning and drug abuse (Koob and Volkow 2010, Ikemoto 2005,
23 2003, Rodd-Henricks et al. 2002). Therefore, we focused on the pathway made up of VTA DAergic
24 projection and the mOT (VTA (DAergic)-mOT) to test our hypothesis that it plays a key role in the
25 formation of odor-preference and the other reward behaviors.

26 In attempting to answer these questions, we first confirmed the direct DAergic projection from VTA to

1 the mOT by using virus-based tracing system. Using fiber photometry recording, we subsequently showed
2 that the activities of the VTA-mOT DAergic projection and the mOT can be changed by reward or odor
3 stimulation respectively. Besides, optogenetic activation of the VTA (DAergic)-mOT pathway was able to
4 activate multiple brain regions and form space/location preferences (even overcame the aversion to central
5 zone). Further, coupling this activation with odor stimulation simultaneously could not only generate
6 preference for a neutral odor, but also abolished the avoidance for an aversive odor. On the other hand,
7 inactivating the mOT-projecting VTA DAergic neurons, or blocking the dopamine receptors in the mOT,
8 abolished the expression of previously formed odor-preferences. These results demonstrate that activation of
9 the VTA (DAergic)-mOT pathway generates odor-preference as well as the other types of preferences. Thus
10 this pathway might be a key player in modulating perception of a given stimulus.

11 **Results**

12 **Mapping the Input Network of the mOT**

13 To map the direct inputs of the mOT, a recombinant RV expressing green fluorescent protein (RV-dG-GFP)
14 was injected into the mOT (Figure 1A, B). RV-labeled neurons were widely distributed in the olfactory
15 systems including the OB, PCX (Figure 1C-F), and entorhinal cortex (data not shown), as well as reward
16 related brain regions such as a large area of the VTA (Figure 1G). In the OB, a large number of neurons in
17 the mitral cell layers as well as a small number of neurons in the external plexiform layer were labeled by
18 RV (Figure 1D, E). Besides, RV also labeled many neurons in other brain regions including the hippocampus
19 and dorsal raphe (data not shown). Our findings are consistent with previous studies that the mOT is
20 connected with both olfactory and reward systems (Ikemoto 2007, Wesson and Wilson 2011), but with more
21 certainty by excluding the possibility of labeling the passing-by fibers.

22 We then examined the cell types of RV infected neurons in the VTA by immunochemical staining of the
23 tyrosine hydroxylase (TH), a biomarker of DAergic neurons, and found about half of the GFP labeled cells
24 (55.32%, n= 3 mice) were TH positive (Figure 1H-J).

1 **The VTA-mOT DAergic Projection Responded to Naturalistic Reward**

2 Both the OT neurons and the VTA DAergic neurons play roles in reward processing (Gadziola et al. 2015,
3 Hu 2016). Although the mOT is densely innervated by the VTA DAergic neurons, the specific functions of
4 this pathway in rewarding have not been tested *in vivo*. Thus, we used calcium dependent fiber photometry
5 (Gunaydin et al. 2014) to detect the VTA-mOT DAergic projection responding to naturalistic reward
6 stimulations in free moving mice.

7 Energy is the basic requirement for the survival of animals, so we first detected the response of this
8 pathway in water- or food-deprived mice to sucrose solution and solid food pellet, respectively. For this
9 purpose, we infused AAV-DIO-GCaMP6m into the VTA of DAT-Cre mice, and recorded the fluorescence
10 signals of the VTA-mOT DAergic terminals (Figure 2A). When the mice sought and acquired sucrose
11 solution, the GCaMP fluorescence was reliably increased ($P < 0.001$, t-test, $n = 6$, Figure 2B-D-left).
12 Sweetened water mainly provides a taste reward, while solid food is a reward related to multiple sensory
13 systems. We then tested the solid food intake and found that the GCaMP signals were also reliably increased
14 with food pellet consumption ($P < 0.001$, t-test, $n = 5$, Figure 2D-middle).

15 In addition, social interaction is critical for animals, we then investigated whether the VTA-mOT
16 DAergic projection is involved. We examined the effect of male-female and male-male interactions, and
17 observed reliable increases of GCaMP fluorescence individually. Because no significant difference of
18 fluorescence changes were observed between the male-female and male-male social interactions, we pooled
19 the data of social interaction experiments ($P < 0.001$, t-test, $n = 6$, Figure 2D-right). For control mice in all
20 the fiber photometry experiments ($n = 3$), only small random signals were observed (Figure 2B, D).

21 Since freely behaving mice refused to consume bitter food or water, to compare the response of the
22 VTA-mOT DAergic projection between reward and aversive stimulus, the sucrose or quinine solutions were
23 orally delivered to head-fixed mice directly through a metal cannula. We found that the VTA-mOT DAergic

1 projection showed a higher response to reward stimuli compared with aversive ones (Figure 2-figure
2 supplement 1).

3 **The mOT Activated by Odor Stimulation**

4 Since the OT has been considered as a component of the olfactory system and the mOT receives direct
5 inputs from the OB (Figure 1C-E), we next tested whether the mOT responds to different kinds of odor
6 stimulations. To verify that the mOT activities can be activated by odor stimulations, we infused
7 AAV-hsyn-GCaMP6s into the mOT of C57BL/6J mice. Calcium signals of the mOT neurons evoked by
8 different odor stimulations were recorded from head-fixed mice (Figure 2-figure supplement 2A). It was
9 found that the mOT neurons were generally activated by different odor stimulations, including isoamyl
10 acetate (ISO), carvone (CAR), citral (CIT), and geraniol (GER), respectively (Figure 2-figure supplement
11 2B). The results demonstrated that the mOT was indeed involved in olfactory functions, which are both
12 consistent with and complement to previous studies using immunohistological and electrophysiological
13 methods (Gadziola et al. 2015, Carlson, Dillione, and Wesson 2014), irrespective of the odor types.

14 **Opto-stimulation of the VTA-mOT DAergic Projection Elicited Reward Behaviors**

15 We showed that the VTA-mOT DAergic projection is activated by diverse naturalistic rewards, but the
16 behavioral effects elicited by the activation of this pathway are still unknown. To selectively manipulate this
17 pathway, we injected AAV9-EF1a-floxed-ChR2-mCherry into the VTA of DAT-Cre transgenic mice (Figure
18 3A). Six weeks after viral infection, we observed mCherry expression in the somas of the VTA neurons
19 (Figure 3-figure supplement 1A, bottom), as well as dense mCherry-positive axon fibers in the mOT (Figure
20 3B). The negative mCherry signal in the VTA of C57BL/6 mice (Figure 3-figure supplement 1A, top) with
21 the same injection indicated that ChR2-mCherry would only express in Cre-positive DAergic neurons in
22 DAT-Cre mice. To further verify the specificity of ChR2-mCherry expression in the DAergic neurons of the
23 VTA, we quantified the number of the VTA neurons that were TH-positive (TH+) and mCherry-positive

1 (mCherry+). We found that about 94.39% of the mCherry+ neurons were also labeled with TH (Figure
2 3C-E), suggesting that the expression of ChR2-mCherry is largely restricted to DAergic neurons. Whole cell
3 recording of light-evoked activity from ChR2-expressing cells in brain slices from these mice revealed that
4 20 Hz blue light pulses reliably induced action potentials in ChR2-expressing neurons (Figure 3-figure
5 supplement 1B). These results laid the basis for further optogenetic manipulation of the DAergic VTA-mOT
6 projection.

7 We then implanted optic fibers at the mOT to activate the VTA-mOT DAergic projection (Figures 3G,
8 H). To reveal the brain regions responding to the activation of the pathway, we screened the c-fos expression
9 (Bepari et al. 2012, Herrera and Robertson 1996, Worley et al. 1993) in brain regions of the olfactory
10 cortexes and reward related areas. As expected, the OT showed a robust enhancement of c-fos activation
11 (Figure 3F, Figure 3- figure supplement 1C. $P = 0.040$, t-test), suggesting that it was strongly activated by
12 stimulation of this pathway. In addition, the c-fos expression was significantly increased in the NAc and
13 PCX compared to the control mice (Figure 3F, Figure 3- figure supplement 1D. $P = 0.006$ for NAc, $P =$
14 0.006 for PCX, t-test). The dorsal striatum (dSTR) and the lateral septal complex (LSX) exhibited a
15 decreased and increased tendency of c-fos expression, respectively, although neither was significant (both $P >$
16 0.05 , t-test). These results indicated that both the reward and the olfactory systems were affected by the
17 activation of the VTA-mOT DAergic fibers.

18 After we confirmed that the VTA-mOT DAergic projection and the mOT are involved in rewards as
19 well as olfaction, and activating of this pathway affects both the reward and the olfactory system, we tested
20 the hypothesis that activation of this pathway might produce odor and even other preferences. For this
21 purpose, we first activated the VTA-mOT DAergic projection to test whether it was able to generate reward
22 behaviors. Real-time place preference (RTPP) tests revealed that mice expressing ChR2 exhibited significant
23 preference for the light-paired chamber ($76.55\% \pm 1.25\%$, $n = 7$), compared with the control mice ($50.22\% \pm$

1 5.27%, n = 7) which only expressed mCherry (P = 0.001, t-test, Figure 3I-K). These data suggested that
2 acute activation of the VTA-mOT DAergic projection produces rewarding effects.

3 Activation of the VTA-mOT DAergic projection induced acute place preference, is this rewarding
4 effect strong enough to overcome the instinctive avoidance and drive positive reinforcement? Tests with
5 intra-Cranial light administration in a specific subarea (iClass, Figure 4A) exhibited that optic activation of
6 mice expressing ChR2-mCherry (n = 7) dramatically increased center exploration, represented by the
7 significantly enhanced entry and retention times, immediately after the first day of iClass training using 20
8 Hz light pulses (Figure 4B-F, P = 0.017 for center entry times, P = 0.017 for center duration in L1; Video 1-5,
9 t-test). We segmented the 15 min training course each day into every 3-min sections, and found that mice
10 rapidly overcame their instinctive avoidance for the central area in about 6 min from light activation in L1
11 (Figure 4D). The preference of mice for the light-paired central area increased with light training ($2.76 \pm$
12 1.08 , 14.81 ± 4.00 , 35.34 ± 6.04 and 52.03 ± 5.27 central entry times; $13.29\% \pm 5.76\%$, $42.29\% \pm 11.49\%$,
13 $78.86\% \pm 9.11\%$, and $85.86\% \pm 9.79\%$ central retention for Pre, L1, L2 and L3, respectively), and was still
14 maintained 24 h later when no light pulse was delivered (33.80 ± 4.23 for central entry times, P < 0.001;
15 $66.86\% \pm 5.66\%$ for central retention, P < 0.001, t-test). No such effects were observed in the control mice
16 (Figure 4B-E, all P > 0.05, n = 7, t-test). The data suggest that activation of the VTA-mOT DAergic
17 projection is able to overcome the instinctive avoidance and drive positive reinforcement.

18 **Opto-stimulation of the VTA (DAergic)-mOT Pathway Coupled with Odor Exposure Elicited** 19 **Odor-preference**

20 We then tested whether activation of the VTA-mOT DAergic projection influences odor-preference. After two
21 days of simultaneous pairing of optical stimulation in the mOT with odor stimulation, mice were tested for
22 preference between the two odors on the following day without light activation (Figure 5A, B). As shown in
23 Figure 5C, we chose one pair of odors (carvone and geraniol), each of them is equivalently sampled by naive

1 mice, and found that the Chr2-expressing mice showed a higher percentage of investigation time to the paired
2 odor (geraniol) compared with the non-paired (carvone) ($P = 0.012$, $n = 8$, t-test, Video 6) or the control mice (P
3 $= 0.053$, $n = 8$, t-test), while the two odors still remained equivalently sampled by the control mice after pairing
4 with optical stimulation ($P = 0.575$, $n = 8$, t-test). These results indicated that activation of the VTA-mOT
5 DAergic projection can elicit odor-preference.

6 As the carvone and geraniol are equivalently sampled by mice inherently, we further tested whether it is
7 possible to abolish or reverse the instinctive aversion to an odor when pairing it with this projection stimulation.
8 We chose two other odors, a preferred (sesame butter) and an aversive (TMT) odor to mice (Kobayakawa et al.
9 2007). After two days of optical stimulation in the mOT pairing with TMT sampling, mice were tested on the
10 following day without light activation. As shown in Figure 5D, after pairing, the Chr2-expressing mice ($n = 8$)
11 spent a significantly higher percentage of investigation time for TMT, compared with the control mice ($P = 0.049$,
12 $n = 8$, t-test) and unpaired odor ($P = 0.025$, t-test), reaching the level equivalent to sesame butter ($P = 0.680$, $n =$
13 8). These results indicate that activation of the VTA-mOT DAergic projection can also abolish the avoidance of
14 mice to an innately aversive odor.

15 However, optical stimulation of the VTA-mOT DAergic projection might lead to the activation of the
16 passing-by DAergic fibers in the mOT or VTA DAergic cell bodies, which may then activate afferents
17 projecting to the other brain regions. To exclude these possibilities and address the role of the local mOT
18 dopamine release in producing the odor-preference, we infused the D1 and D2 dopamine receptor
19 antagonists (SCH-23390 and raclopride) 5-min before pairing the projection activation with odor stimulation
20 (Figure 5E). We found that administration of these drugs abolished the formation of preference for the paired
21 odor (Figure 5F, $P = 0.757$, $n = 6$, t-test), which is preferred by animals with only saline infusion (Figure 5F,
22 $P = 0.027$, $n = 6$, t-test). These results indicated that the local mOT dopamine released by the VTA
23 (DAergic)-mOT pathway is responsible for the formation of odor-preference as we have observed.

1 We have shown that it is sufficient to generate odor-preference by activating the VTA (DAergic)-mOT
2 pathway while exposed to the odor simultaneously, and that dopamine in the mOT is necessary for this
3 process. However, the potentially supra-physiological activation produced by optogenetic manipulation
4 might elicit artificial behaviors. Therefore, whether this pathway is really necessary for the formation of
5 odor-preference under the influence of hedonic life experience still remains unclear. Further, whether or how
6 this pathway plays roles in the perception of the preferred odors after the formation of odor-preference is
7 also unknown. To address these questions, we decided to train water deprived mice for Go-no go task, with
8 one of the two odors associated with water, a naturalistic reward, then examine the effects caused by the
9 chemogenetical inactivation of the mOT-projecting VTA DAergic neurons. At first, we co-injected
10 RV-dG-GFP into the NAc and RV-dG-dsRed into the mOT (Figure 6A, B), and found that the co-labeled rate
11 (1.65%) of the VTA neurons were negligible, which implied that it may not be common for a VTA DAergic
12 neuron to co-innervate the NAc and the mOT (Figure 6C-E). Thus, we are able to selectively target the
13 mOT-projecting VTA DAergic neurons, and further express hM4Di in these neurons (Figure 7A, C) to
14 silence them. To achieve this goal, we injected CAV-CMV-Cre and AAV9-EF1a-floxed-hM4Di-mCherry or
15 AAV9-EF1a-floxed-mCherry into the mOT and VTA, respectively in C57BL/6 mice (Figure 7A). The
16 mCherry positive cells are restricted to the VTA area (Figure 7B, C), and the projections in the OT are
17 mainly distributed in the medial part (Figure 7D). We found that although the mCherry-positive cells only
18 took a small portion (37.20 %) of the whole VTA DAergic neurons (Figure 7-figure supplement 1A, B),
19 most (90.86 %) of the mCherry labeled cells were also co-expressing TH (Figure 7E, F). The ratio of
20 co-labeled TH⁺ neurons produced by CAV is much higher than by RV-infection (Figure 1J). Since the
21 expression of endogenous proteins are often severely reduced followed by RV infection, the lower
22 co-labeling ratio for RV might be underestimated. Thus, with CAV-CMV-Cre retrograde transport from the
23 mOT, we are able to selectively silence the mOT-projecting VTA DAergic neurons. We found that after the

1 Go-no go training was performed, inactivating the mOT-projecting VTA DAergic neurons disrupted the
2 conditioned odor-preference (Figure 7G), but intact odor discrimination remained (Figure 7H, left and
3 middle bar pairs). These results indicated that the projection might be necessary for established
4 odor-preference but not critical for odor discrimination. We further found that when the mOT-projecting
5 VTA neurons were inactivated during the Go-no go training, the learning efficiency of the well-trained mice
6 to a new odor pair was strongly affected (Figure 7H, right bar pair, 66.17% accuracy vs. 91.00% for control,
7 with random level at 50%, $P=0.002$), suggesting the important roles of the projection to establish the
8 paradigm which can lead to the formation of odor-preference.

9 Moreover, we found that dense axonal fibers were also distributed in the NAc for some mice, which
10 was not consistent with the RV labeled results (Figure 6). This might be caused by the large amount of
11 CAV-CMV-Cre injected into the mOT, which may diffuse into the nearby regions. To exclude the possibility,
12 we injected the AAV9-EF1a-floxed-eNpHR3.0-mCherry into the VTA of DAT-Cre mice and bilaterally
13 inactivated the VTA-mOT DAergic projection in an odor-food associative learning test (Figure 8A-C). The
14 control mice showed a significant preference to the S+ odor after the learning session (Figure 8D, $52.43\% \pm$
15 5.32% for pre learning, $67.78\% \pm 3.40\%$ for post learning, $P=0.018$). However, optogenetic inhibiting the
16 VTA-mOT DAergic projection during the odor-food associative learning disrupted the conditioned
17 odor-preference of the eNpHR-expressing mice (Figure 8D, $51.82\% \pm 2.66\%$ for pre learning, $57.07\% \pm$
18 3.06% for post learning, $P=0.134$).

19 Together, these results indicated that the VTA-mOT DAergic projection should play important roles in
20 the formation of odor-preference under the influence of hedonic life experience.

22 Discussion

23 The OT has been implicated in both reward and olfactory information processing (Wesson and Wilson

2011). In the present study, we first showed that various types of odors and diverse naturalistic of reward stimulations can activate the mOT and the VTA-mOT DAergic projection, respectively. Then we found that activation of the VTA (DAergic)-mOT pathway can generate preference for a neutral odor or abolish the avoidance for an aversive odor; inhibition of the projection downstream in the mOT through specific dopamine receptor antagonists prevented odor-preference formation completely; and inactivation of the mOT-projecting VTA DAergic neurons fully blocked the formed odor-preference, and strongly attenuated the Go-no go learning performance which leads to the odor-preference established through naturalistic reward odor-preference. These data suggest that the VTA (DAergic)-mOT pathway mediates the formation of odor-preference.

VTA-mOT DAergic Projection in Reward

Although previous study has shown that electrical stimulation of the OT promotes reward (FitzGerald, Richardson, and Wesson 2014), the behavioral effects have never been evaluated by directly targeting the VTA-mOT DAergic projection. It is reported that the ventral striatum is heterogeneously innervated by GABAergic, glutamatergic and DAergic afferents from the VTA. DAergic neurons in the VTA are involved in diverse functions, depending on their projection targets (Kim et al. 2016, Cohen et al. 2012). The roles of the VTA-mOT DAergic projection still remain unclear. Here, using optogenetics, we found that, activation of the VTA-mOT DAergic projection elicited RTPP (Figure 3G-K) (Stamatakis and Stuber 2012), and the rewarding effect was strong enough to rapidly overcome the instinctive avoidance of mice to drive positive reinforcement (Figure 4). Moreover, taking advantage of *in vivo* calcium dependent fiber photometry, we found for the first time that the VTA-mOT DAergic projection was activated by diverse naturalistic rewards, including sucrose solution, solid food and social interactions (Figure 2). Our results consolidate the rewarding role of the mOT and demonstrate that the VTA-mOT DAergic projection is involved in this function.

Lacking cellular specificity, electrical stimulation might activate local neuron population, and axon fibers projecting to the area and passing-by non-selectively. Therefore, it was difficult to decide which component(s), local neurons, afferent to or efferent from the OT, and fibers passing-by the OT, contribute to

1 the observed effects. Our results using optogenetics proved that activation of the VTA-mOT DAergic
2 projection contributes to the rewarding role of the mOT, though the downstream neurons in the mOT
3 involved in this pathway still need to be elucidated. It was reported that activation of the trimeric G-protein
4 Gs-coupled D1R increases the excitability of the D1R+ neurons, and that activation of the Gi-coupled D2R
5 decreases the excitability of the D2R+ neurons (Stoof and Keabian 1981). Thus, the rewarding effect
6 observed here might be due to the simultaneous activation of D1R+ neurons and inhibition of D2R+ neurons
7 followed by dopamine release in the mOT. Besides, cholinergic neurons in the OT also respond to DAergic
8 terminal activation (Wieland et al. 2014), which might also lead to reward, because rats easily learned to
9 self-administer cholinergic receptor agonists carbachol in the NAc (Ikemoto et al. 1998). Together, these
10 researches implicated that the rewarding effects produced by stimulation of the VTA-mOT DAergic
11 projection might be the results of diverse activation and/or inactivation response of different populations of
12 neurons in the mOT. Further studies using optogenetic and chemogenetic to manipulate cell-type specific
13 neurons in the mOT with corresponding Cre-line transgenic mice for the elucidation of the downstream
14 pathway would be of great interest.

15 On one hand, artificial activation of the VTA-mOT DAergic terminals generates reward behavior; on the
16 other hand, this pathway is activated by naturalistic rewards, including sucrose solution, solid food and
17 social interactions. It is reported that the activities of the VTA DAergic projection are target-dependent in
18 response to rewards and shock (Kim et al. 2016). For example, the projection to NAc has been shown to
19 increase activity during reward and decrease activity during shock, while the projection to
20 basolateral-amygdala displayed increased response to both reward and shock. Also, the projection to
21 prefrontal cortex exhibited increased activity to shock but not reward. We found that the VTA-mOT DAergic
22 projection is activated by different types of naturalistic rewards, thus suggesting that it might mediate
23 generalized rewarding processes. Besides, the VTA-mOT DAergic projection is also slightly activated by the
24 bitter quinine solution, although it is more weakly activated than by sucrose solution. Furthermore, although
25 the NAc/mOT-projecting VTA DAergic neurons may hardly be completely labeled limited by the efficiency
26 of RV infection, it could be speculated that the VTA DAergic neurons may not commonly innervate both the

1 NAc and mOT depending on the very low co-labeled rate of VTA neurons by RV (Figure 6). These results
2 added new information to the functional heterogeneity of VTA DAergic projections.

3 **VTA (DAergic)-mOT Pathway in Odor and Other Preferences**

4 Reward-related odor perception is critical for survival and reproduction of animals (Doty 1986). As recent
5 studies have shown that the OT neurons encode odor valence by enhancing firing rates (Gadziola et al.
6 2015), and that rewarding odor cues preferentially activate the D1R+ neurons in the mOT (Murata et al.
7 2015), the mOT seems to be involved in odor-preference. However, the mechanism of how the
8 odor-preference is established under the influence of life experience remains unclear.

9 In the present study, we found that the VTA-mOT DAergic projection is activated by diverse
10 naturalistic rewards, the activities of the mOT are altered by a wide range of odorants, and mice exhibited a
11 preference for a given odor if that olfactory stimulant is paired with the activation of the VTA
12 (DAergic)-mOT pathway. Our results thus provide an insight that the activation of the VTA-mOT DAergic
13 projection by hedonic life experience might contribute to the generation of the preference for experience
14 related odors.

15 We showed that it is sufficient to artificially generate odor-preference by optogenetic activation of the
16 VTA-mOT DAergic projection (Figure 5). Since this phenomenon is abolished by the dopamine receptor
17 antagonist administration in the mOT, and it may not be common for a VTA DAergic neuron to co-innervate
18 the NAc and the mOT (Figure 6), we can exclude the contributions of the activation of passing-by DAergic
19 fibers in the mOT or VTA DAergic cell bodies, and confirm that the mOT dopamine released by the
20 VTA-mOT DAergic projection should be responsible for this odor-preference formation. Besides, this
21 pathway is also necessary for odor based reward learning and the expression of naturalistically formed
22 odor-preference (Figure 7, 8). However, whether or how this pathway plays roles in the formation of odor
23 aversion, or the perception of the instinct preferred/aversive odors is still unknown.

24 In the present study, inactivating the mOT projecting VTA neurons did not affect the learnt Go-no go
25 performance (Figure 7G, H), mice were both highly motivated and still remembered how to seek water
26 rewards. The possible reasons are that, the limited population of DAergic neurons labeled by CAV-CMV-Cre

1 from the mOT may lead to incomplete inhibition or alternatively, the specific VTA (DAergic)-mOT pathway
2 might not be necessary for established reward seeking behavior. Thus, the other neural pathways such as the
3 different populations of VTA DAergic neurons projecting to the NAc, dorsal striatum and other brain regions
4 may compensate the motivation and expression of reward seeking (Hu 2016).

5 Inactivating the mOT projecting VTA neurons did not affect reward seeking, but strongly affected the
6 learning efficiency for a new odor pair. Dopamine has been widely reported to strengthen environment
7 stimuli-encoded glutamate inputs in the NAc, thus facilitated environment cue-based reward learning (Flagel
8 et al. 2011, Britt et al. 2012). However, the function of the VTA (DAergic)-mOT pathway in reward
9 learning has been rarely studied. Here we reported that the pathway plays important roles in odor cue-based
10 reward learning, toward which mice are able to establish an odor-preference. Since inactivating the mOT
11 projecting VTA neurons abolished the preference for S+ odor, together, we summarized that the VTA
12 (DAergic)-mOT pathway is both necessary for the expression of established odor preference and may
13 influence the establishment of odor-preference.

14 The reasons why paired activation of the VTA-mOT DAergic projection generates odor-preference
15 could be complex. Given that the mOT is directly innervated by mitral/tufted cells from the OB (Figure
16 1;(Igarashi et al. 2012, Scott, McBride, and Schneider 1980)) and participates in odor perception (Figure
17 2-figure supplement 2); (Agustin-Pavon, Martinez-Garcia, and Lanuza 2014, Mooney et al. 1987, Carlson,
18 Dillione, and Wesson 2014)), and that the D1R+ neurons in the mOT are involved in reward related odor
19 perception, the first possibility is that activation of the VTA-mOT DAergic projection might induce
20 long-term potentiation (LTP) in mOT D1R+ neurons, and enhance the paired odors related input connections
21 with these neurons. Hence, future occurrences of the paired odors should result in an increased rate of
22 activation of D1R+ neurons in the mOT, even without artificial activation of the VTA-mOT DAergic
23 projection, as is the case in the NAc (Keeler, Pretsell, and Robbins 2014, Gerfen and Surmeier 2011, Hikida
24 et al. 2010). Another possibility involves a broader network. In the present study, we found that activating
25 the VTA-mOT DAergic projection induced increased c-fos expression in both the NAc and PCX (Figure
26 3A-F, Figure 3-figure supplement 1). Because the NAc is involved in reward (Hu 2016, Carlezon and

1 Thomas 2009) and the PCX is responsible for olfactory memory and odor perception (Wilson and Sullivan
2 2011), it's likely that the simultaneous activation of these two and the other brain regions may refer the
3 olfactory memory of the paired odors to reward, leading to altered odor-preference. Further studies with
4 specific manipulation and recording of neurons in the mOT and PCX are needed to address the mechanism
5 in detail.

6 Animals learn to associate diverse sensory cues, not only odors, with rewards depending on their life
7 experience. The striatum plays an important role in experience-dependent reward learning behaviors (Mahon,
8 Deniau, and Charpier 2004, Wickens, Reynolds, and Hyland 2003). Blockade of the striatum D1R+ neurons
9 damages both the visual cue-based reward learning and cocaine-induced conditional place preference
10 (Yawata et al. 2012, Hikida et al. 2010). Besides, the activation of striatum D1R is necessary for the
11 generation of corticostriatal LTP that induced by concurrent phasic dopamine release and cortical stimulation
12 (Keeler, Pretsell, and Robbins 2014, Mahon, Deniau, and Charpier 2004). Visual, auditory and other sensory
13 cues can usually stimulate the cortical activation. As a part of the ventral striatum, the OT neurons also
14 respond to an auditory stimulus (Wesson and Wilson 2010). It's pleasant for pet dogs to hear the voice of
15 their owners and for lovers to hear the melodies of the songs they sang together. Whether the VTA-mOT
16 pathway influences these auditory preferences is also an interesting question.

17 **The Functional Differences between the mOT and the Adjacent Brain Regions**

18 The OT is composed of the medial and lateral parts, which are functionally different from each other
19 (Murata et al. 2015, DiBenedictis et al. 2015, Agustin-Pavon, Martinez-Garcia, and Lanuza 2014, Ikemoto
20 2003). Thus, how the VTA DAergic projection to the lateral OT affects and responds to reward or aversion
21 compared with the mOT still remains to be examined.

22 It should also be pointed out that, although we intended to reveal the functions of the VTA-mOT
23 DAergic projection in odor-preference, the border for the mOT and the lateral OT could be potentially
24 imprecisely divided due to limited knowledge about this. Besides, it's also a difficult problem to perfectly
25 demark the OT from the ventral pallidum. In the present work, we divided the mOT from the lateral OT at
26 the most gyrated part of the layer 2 as we did before (Zhang et al. 2017), and assigned the mOT with the

1 region containing the superficially located Islands of Calleja and surrounded cortex-like compartments
2 according to the previous reports (Murata et al. 2015, Xiong and Wesson 2016). Besides, the layers of the
3 OT were also divided using methods in Xiong's work (Xiong and Wesson 2016). The border of the layer 3
4 was demarked by the deep layer's islands of Calleja.

5 Besides, the NAc and OT, components of the ventral striatum, mediate reward processing similarly
6 (Striano et al. 2014, Millhouse and Heimer 1984) and both are innervated by DAergic projections from the
7 VTA. Although the NAc has been extensively studied, the OT has received much less attentions, in spite of
8 the unique anatomical position. Previous studies found that the mOT robustly mediates self-administration
9 of cocaine or D-amphetamine more than the NAc (Ikemoto 2005, 2003). Given that pharmacological agents
10 can diffuse easily, it is difficult to specifically target the mOT while leaving the adjacent brain areas (like the
11 NAc) undisturbed. Meanwhile, a recent research reported that optogenetic activation of DAergic terminals
12 innervating the NAc is sufficient to drive positive reinforcement (Steinberg et al. 2014), whether there
13 would be any functional difference between activation of DAergic projection in the mOT and NAc is
14 unknown. Further studies using optogenetic activation of VTA DAergic projections in the NAc might be of
15 great help to reveal their features.

16 In summary, we have provided evidence that the VTA-mOT DAergic projection can be activated by a
17 variety of rewards and that activation of the projection can generate robust rewarding, leading to formation
18 of olfactory as well as spatial preferences if the corresponding stimulation is coupled with the activation of
19 the projection simultaneously. These results may underlie a circuit mechanism for how preference is
20 influenced by life experience.

22 **Materials and Methods**

23 **Animals**

24 All surgical and experimental procedures were conducted in accordance with the guidelines of the Animal
25 Care and Use Committees at the Wuhan Institute of Physics and Mathematics, the Chinese Academy of
26 Sciences (reference number: WIPM-(2014)39). Adult male and female C57BL/6 mice were purchased from

1 Hunan SJA Laboratory Animal Company. DAT-Cre mice used were heterozygote and bred from
2 DAT-internal ribosome entry site (IRES)-Cre (Jackson Laboratories, B6.SJL-Slc6a3tm1.1 (Cre) Bkmn/J,
3 stock number 006660) (Backman et al. 2006) by mating the transgenic male mice with C57BL/6 females.
4 All animals were housed with their littermates in a dedicated housing room with a 12/12 h light/dark cycle.
5 Food and water were freely available unless specifically noted.

6 **Viral Constructs**

7 For AAV viruses, the AAV9-EF1a-floxed-ChR2-mCherry, AAV9-EF1a-floxed-eNpHR3.0-mCherry,
8 AAV9-EF1a-floxed-hM4Di-mCherry, AAV9-hsyn-Gcamp6s, and AAV9-EF1a-floxed-mCherry were
9 packaged by BrainVTA Co., Ltd., Wuhan. AAV9-EF1a-DIO-GCaMP6m and AAV9-EF1a-DIO-EmGFP
10 were gifts from Minmin Luo and constructed by replacing the coding region of ChR2-mCherry in the
11 AAV9-EF1a-DIO-hChR2(H134R)-mCherry plasmid (constructed by K. Deisseroth) with those encoding
12 enhanced membrane GFP (Addgene Plasmid 14757) or GCaMP6m (Addgene Plasmid 40754), respectively.
13 All AAVs were purified and concentrated to titers of approximately 2×10^{12} genome copies per milliliter.

14 For rabies viruses, the RV-dG-GFP and RV-dG-dsRed were packaged by standard methods as previous
15 described (Osakada et al. 2011) with titers at about 1×10^9 pfu/ml.

16 To specifically inactivate the mOT-projecting VTA DAergic neurons, CAV-CMV-Cre was also
17 packaged at titers of approximately 3×10^{12} genome copies per milliliter by BrainVTA Co., Ltd., Wuhan.

18 **Stereotactic Surgery**

19 All procedures on animals were performed in Biosafety level 2 (BSL2) animal facilities as we did before
20 (Yang, Yang, et al. 2016, Yang, Wang, et al. 2016). Briefly, animals were anesthetized with chloral hydrate
21 (400 mg/kg, i.p.), and then placed in a stereotaxic apparatus (RWD, 68030). During surgery and virus
22 injection, animals were kept anesthetized with isoflurane (1%). The skull above the targeted areas was
23 thinned with a dental drill and removed carefully. Injections were conducted with a syringe pump
24 (Quintessential stereotaxic injector, Stoelting, Cat#: 53311) connected to a glass micropipette with a tip
25 diameter of 10-15 μ m.

26 To retrograde trace the afferent neural circuit of the mOT, RV-dG-GFP (150 nL) was unilaterally

1 injected into the mOT of the adult male C57BL/6 mice with the following coordinates: AP, 1.20 mm; ML,
2 1.10 mm; and DV, -5.50 mm. 7 days after virus injection, subjected mice were sacrificed.

3 To label the co-innervation of VTA neurons to the mOT and NAc, we co-injected 100 nL RV-dG-dsRed
4 into the mOT and RV-dG-GFP into the NAc with the following coordinates: AP, 1.50 mm; ML, 0.7 mm; and
5 DV, -4.50 mm. 7 days after virus injection, subjected mice were sacrificed.

6 To specifically manipulate and record the activities of the VTA-mOT DAergic projection, we
7 respectively injected 300 nL of AAV9-EF1a-floxed-ChR2-mCherry,
8 AAV9-EF1a-floxed-eNpHR3.0-mCherry or AAV9-EF1a-floxed-mCherry, AAV9-EF1a-DIO-GCaMP6m or
9 AAV9-EF1a-DIO-EmGFP into the VTA of adult DAT-Cre mice with the following coordinates: AP,
10 -3.20 mm; ML, 0.45 mm; and DV, -4.30 mm. Eight weeks later, subjects were ipsilaterally or bilaterally
11 implanted with a chronic optical fiber (NA = 0.37, Φ = 200 μ m; Fiblaser, Shanghai, China) or a cannula (OD
12 = 0.48 mm, ID = 0.34 mm, RWD, 68030) targeted to the mOT with the following coordinates: AP, 1.20 mm;
13 ML, 1.10 mm; and DV, -5.15 mm.

14 To specifically record the activities of the mOT neurons, we ipsilaterally injected 150 nL of
15 AAV9-hsyn-Gcamp6s into the mOT of male C57BL/6J mice with the following coordinates: AP, 1.20 mm;
16 ML, 1.10 mm; and DV, -5.50 mm. Two weeks later, subjects were implanted with a chronic optical fiber
17 targeted to the mOT with the following coordinates: AP, 1.20 mm; ML, 1.10 mm; and DV, -5.15 mm.
18 Implants were fixed to the skull using two small screws, Cyanoacrylate Adhesive (Tonsan Adhesive, Beijing,
19 China) and followed by dental cement (New Century, Shanghai, China). After the surgery, lincomycin
20 hydrochloride and lidocaine hydrochloride gel were applied to the incision sites to prevent inflammation and
21 decrease pain. Mice were allowed to recover for at least 1 week before behavioral tests. Brain sections
22 containing the mOT (AP from about 1.40 mm to 0.60 mm) were collected to confirm the site of optical fiber.

23 To specifically inactivate the mOT-projecting VTA DAergic neurons, 250 nL of CAV-CMV-Cre was
24 bilaterally injected into the mOT of adult male C57BL/6 mice with the same coordinate as above, and 300
25 nL of AAV9-EF1a-floxed-hM4Di-mCherry or AAV9-EF1a-floxed-mCherry into the VTA of the C57BL/6
26 mice with the following coordinates: AP, -3.20 mm; ML, 0.45 mm; and DV, -4.30 mm. About 3 weeks later,

1 subjects were implanted with a small home-made metal bark to the skull for head-fixed Go-no go training.

2 **Odor Stimulation**

3 For the odor stimulation, isoamyl acetate, carvone, citral, and geraniol (all from Sigma, MO, USA)
4 with 5% dilutions of saturated vapors were used. And mineral oil was used as a control. Each odor was
5 presented for four consecutive trials. The duration of the odor pulse was 2 s with an inter-trial interval of 28
6 s to prevent habituation. Verification of the optic fiber placement were done at the end of the experiments,
7 using methods described in our previous publication (Li, Gong, and Xu 2011).

8 **Optogenetic Manipulations**

9 **Slice Recording**

10 The DAT-Cre mice with AAV9-EF1 α -DIO-ChR2-mCherry injected into the VTA were used. The mice
11 were anesthetized with isoflurane. After rapid decapitation, the brains were quickly removed and placed into
12 ice-cold oxygenated slicing solution saturated with mixture of 95% O₂ and 5% CO₂. Coronal sections (300
13 μ m thick) of the VTA were acquired using a vibratome (Leica, VT1000S) at 0-4 °C. The slices were
14 incubated at 34 °C for 30 min and then at room temperature (22-24 °C) with oxygenated artificial
15 cerebrospinal fluid (ACSF) consisted of (in mM): 118 NaCl, 2.5 KCl, 2 CaCl₂, 2 MgCl₂, 26 NaHCO₃, 0.9
16 NaH₂PO₄, 11 D-glucose. After incubation, a slice was transferred to the recording chamber, superfused with
17 oxygenated ACSF at a rate of 2 ml/min for recording.

18 Whole cell recording was performed with borosilicate glass pipettes pulled to a tip resistance of 3 to 5
19 M Ω (Sutter Instrument Co., P-1000). Recording electrodes were filled with intracellular solution (in mM):
20 140 K-gluconate, 5 KCl, 2.5 MgCl₂, 10 HEPES, 4 Mg-ATP, 0.4 Na-GTP, 10 Na-phosphocreatine, 0.6
21 EGTA (pH 7.2, osmolarity 290 MOsm). Signals were recorded with a MultiClamp 700B amplifier
22 (Molecular Devices, USA) and digitized at 10 kHz with DigiData 1440A (Molecular Devices, USA). The
23 somas of ChR2-expressing VTA DAergic neurons (mCherry-positive) were easily identified. To optically
24 stimulate ChR2-expressing neurons, a single-wavelength LED system (λ = 470 nm, CoolLED PE-100) with
25 light pulses at 5 ms, 20 Hz was used. Data were analyzed using Clampfit 10.3 software and origin 9.0.

26 **Behavioral Task**

1 For all behavioral experiments, we handled the mice for 2 days before the training experiment, 3-5 min for
2 each day, allowing them to get used to the tethering procedure. For optogenetic stimulation, the implanted
3 optic fiber was connected to a blue light laser *via* patch cords (Fiblaser, Shanghai, China) and a fiber-optic
4 rotary joint (Doric Lenses, Quebec, Canada), which could release the torsion of the fiber resulted from
5 rotation of the mouse. All photo-stimulation experiments used 5 ms, 10-15 mW, 473 nm light pulses at 20
6 Hz *via* a solid-state laser for light delivery (Shanghai Laser & Optics Century, Shanghai, China) triggered by
7 a stimulator (Model 2100, Isolated pulse stimulator, A-M systems).

8 **Real-Time Place Preference (RTPP)**

9 The mice were placed in a behavioral arena ($50 \times 50 \times 25$ cm) for 20 min and assigned one counterbalanced
10 side of the chamber as the stimulation side. Mice were placed in the non-stimulation side at the onset of the
11 experiment. Laser stimulation at 20 Hz were constantly delivered with when they crossed to the stimulation
12 side, but stopped when they returned back to initial non-stimulation side. All behavioral tests were recorded
13 using an HD digital video camera (Sony, Shanghai, China) and the offline analyses were performed by a
14 video tracking software (ANY-maze; Stoelting Co, Illinois, USA).

15 **iClass**

16 The behavioral arena (47×32 cm) contained a red rectangle as the target area for reinforcement, located in
17 the center of the open field. The red central rectangle, formed by border line with the height of about 1 cm,
18 is one-tenth of the whole arena. During the experiment, the floor of the arena was covered by fresh padding,
19 with the red central area easily seen. The behavior task consisted of three phases (pre, light training, and test)
20 and lasted for 5 consecutive days (Liu et al. 2014). During the pre-phase on day 1 (pre), mice with fiber
21 patch cord connected were habituated in the arena without light pulses delivery. The basal locomotor
22 activities of the mice were recorded and measured. The following light training sessions consisted of three
23 consecutive days (L1-L3), on each day mice with fiber patch cord connected were put in the arena, and their
24 activities were monitored for 15 min. When the centrals of the mice were located within the marked central
25 rectangular area, blue light pulses at 20 Hz were constantly delivered into the mOT. Light stimulation was
26 immediately terminated when the centrals of the mice left the red area. On test day (test), the same

1 experimental procedures as in day 1 (pre) were performed.

2 **Odor-light Pairing**

3 The pairing procedure was performed for two consecutive days, which was two weeks post-surgery and
4 plate placement. On each of the pairing days, the mouse was head restrained and adapted to the holding and
5 odorant delivery conditions for 1-2 h. Carvone and geraniol (Sigma, MO, USA) were randomly delivered to
6 the mouse's nose (2 s delivery, 30 s inter-stimulus interval, 20 trials each session for 5 sessions) with 5% of
7 saturated vapors using a custom 8-channel olfactometer and balanced across mice. Only geraniol was
8 delivered simultaneously with 2 s, 20 Hz trains of light pulses (473 nm). Control mice were treated
9 identically. Furthermore, another pair of odors (v/v 5% TMT and sesame butter) was delivered in the same
10 way, with TMT as the paired odor.

11 In the subsequent receptor blockade experiments, saline (200 nL in total) contained the D1R antagonist
12 (SCH-23390, 1.0 mg/ml) and D2R antagonist (Raclopride, 1.5 mg/ml) as blocking agent, or saline alone
13 (200 nL) as control, was administered into the mOT through the cannula 5 min before optogenetic activation
14 of the VTA-mOT DAergic projection paired with odor stimulation, which were described as above.

15 **Odor-food reward associative learning**

16 The protocols were adapted from Sophie's study (Tronel and Sara 2002) with some modifications.
17 Briefly, the investigation time of the mice to the two odors (geraniol and carvone) were measured
18 (odor-preference test), and then mice were fasted 24h pre-training. The training apparatus was a square box
19 with two sponges which had a hole of 1 cm in diameter cut into the center and were placed in glass
20 side-holders of the same size. Two sponges were randomly placed in two opposite corners of the box. Food
21 reinforcement was placed at the bottom of the opening in the sponge. Sponges were impregnated with an
22 odor on each corner of the sponge. Training was performed in a single session with five trials. The mouse
23 was introduced into the box at a corner without a sponge, head toward the wall. The spatial configuration of
24 the sponges was changed between trials and the reinforcement was always associated with the geraniol. The
25 constant 593 nm yellow light were constantly delivered into the mOT once the mouse was introduced into
26 the box and during the training session. After the training was finished, the mice were taken to the

1 odor-preference test.

2 **Odor-preference Test**

3 Mice were tested with the two odors (5% in mineral oil, v/v), applied by two glass sticks simultaneously, to
4 their home cages. Home cage testing was chosen to minimize potential influences of stress and anxiety
5 (because of the new environment/context) on the behavioral measures. The food and water were removed
6 from cages just before tests. Tests took place during the light phase of the animals' 12/12 h dark/light cycle.
7 Odors were delivered for 6 min by inserting the odorized sticks from one side of the animal's home cage.
8 Mice were first habituated to the odor sticks for 1 min, and the time spent investigating, defined as sniffing
9 within 1 cm of the odor stick, was recorded by a single observer blind to the experiment group over a 5 min
10 period.

11 **Go-no go task**

12 After about 24 h of water deprivation, mice were exposed to these two odors randomly. They were trained to
13 either lick the water pipe to get the reward (a drop of water) when they smelled one odor (defined as S+
14 odor), or wait without any licking when presented the other odor (defined as S- odor). After several days of
15 training, when the accuracy reached above 85%, the mice were ready for further experiments. They were
16 intraperitoneally injected with CNO (3 mg/kg of body weight) and then tested for odor-preference blockade
17 experiments. Moreover, in the following days, the mice were trained to distinguish another pair of odors
18 using the same principle they learned before, until the accuracy achieved above 85% again.

19 **Sucrose Solution and Food Pellets Consumption**

20 Mice were water deprived for 24 h before placed in a chamber (20 × 20 × 22 cm), which was equipped with
21 a bottle filled with 5% (w/v) sucrose solution. The lick signals were recorded by a contact lickometer
22 connected with a Power 1401 data acquisition system.

23 Mice were food deprived for 24 h before placed in a chamber (20 × 20 × 22 cm). Food pellets were
24 manually delivered to the chamber floor with only one pellet per time. Videos (10 min per session) from an
25 overhead infrared camera were recorded. The onset of feeding was determined as the mouse picked up the
26 pellet and started chewing.

1 **Social Interaction**

2 To study the effect of heterosexual interaction, the test male mouse was habituated in the dark with an
3 optical fiber connected to the fiber ferrule on its head for 1 min. A female mouse was introduced into the
4 home cage of the test male mouse. A recording session lasted for 10 min and the behavior of the test mouse
5 was videotaped with an overhead infrared camera. In the male-male interaction sessions, a male mouse was
6 introduced following the same procedure.

7 **Fiber Photometry**

8 The GCaMP fluorescent signals for sucrose or quinine solution, food pellets, social interactions and odors
9 were recorded with the same setup (Fiber photometry, Thinker Tech Nanjing Biotech Limited Co.) as
10 previously reported (Li et al. 2016).

11 **Immunohistochemistry**

12 Briefly, 40 μm thick coronal slices were obtained and the procedures for immunohistochemistry were
13 performed similar to what we did before (Wei et al. 2015).

14 To determine the input patterns of the mOT, every sixth sections of the RV labeled brain slices were
15 collected and stained with DAPI. 4 coronal slices from the VTA (AP from about -3.00 mm to -3.80 mm,
16 spaced 240 μm from each other) per mouse were immunohistochemically stained for the tyrosine
17 hydroxylase (TH, Abcam, Lot#: 2552365).

18 To determine the specificity of Chr2-mCherry expression in the VTA of DAT-Cre mice, 4 coronal
19 slices from the VTA (AP from about -3.00 mm to -3.80 mm, spaced 240 μm from each other) per mouse (n =
20 3) were collected and immunohistochemically stained for the TH.

21 To detect the c-fos expression evoked by optical-manipulation, mice were put in an open field and
22 received laser illumination for 10 min, and were sacrificed 1.5 hours later. Every sixth brain sections (AP
23 from about 1.40 mm to 0.50 mm) from 3 mice were collected and immunohistochemically stained for c-fos
24 (Cell Signaling, #2250).

25 All of the images were then captured and analyzed with TCS SP8 fluorescence laser scanning confocal
26 microscope (Leica) and ImageJ software.

1 **Data Analyses**

2 For cell counting, the boundaries of brain regions were delineated manually with Photoshop based on the
3 Allen Brain Atlas. The labeled neurons were quantified semi-automatically using FIJI and the cell counter
4 plugin of ImageJ.

5 For statistical analyses, we first analyzed data from one mouse trial by trial, then calculated the mean
6 value and standard errors of one group, then Independent-Samples T-Test were used to determine statistical
7 differences between groups using SPSS (version 13.0). Statistical significance was set at *** $P < 0.001$; ** P
8 < 0.01 ; * $P < 0.05$. All data values were presented as mean \pm s.e.m. Graphs were made using SigmaPlot
9 (version 10.0).

10 **Funding**

11 This work was supported financially by the National Basic Research Program (973 Program) of China
12 (Grant No. 2015CB755600 to F.X.), Strategic Priority Research Program of Chinese Academy of Sciences
13 (Grant No. XDB02050005 to F.X.), the National Natural Science Foundation of China (Grant No. 31771156,
14 81661148053 and 91632303 to F.X. and Grant No. 31400945 to Q.L, Grant No. 31400946 to X.P.R, Grant
15 No. 31400977 to X.B.H).

16 **Acknowledgements**

17 We thank Shanping Chen from Shenzhen Institutes of Advanced Technology for helping with slice
18 recording, Yanqiu Li from Wuhan Institute of Physics and Mathematics for keeping and genotyping the
19 DAT-Cre mice, Lingling Xu from Wuhan Institute of Physics and Mathematics for capturing confocal
20 images, and Tung-Lin Wu from Vanderbilt University Medical Center (a native English speaker) to modify
21 the manuscript.

22 *Conflict of Interest:* None declared

23

1 References

- 2 Agustin-Pavon, C., F. Martinez-Garcia, and E. Lanuza. 2014. "Focal lesions within the ventral striato-pallidum abolish attraction for
3 male chemosignals in female mice." *Behavioural Brain Research* 259:292-296. doi: 10.1016/j.bbr.2013.11.020.
- 4 Backman, C. M., N. Malik, Y. J. Zhang, L. Shan, A. Grinberg, B. J. Hoffer, H. Westphal, and A. C. Tomac. 2006. "Characterization of a
5 mouse strain expressing Cre recombinase from the 3' untranslated region of the dopamine transporter locus." *Genesis* 44 (8):383-390. doi: 10.1002/dvg.20228.
- 6 Bepari, A. K., K. Watanabe, M. Yamaguchi, N. Tamamaki, and H. Takebayashi. 2012. "Visualization of odor-induced neuronal
7 activity by immediate early gene expression." *Bmc Neuroscience* 13. doi: Artn 140
8 10.1186/1471-2202-13-140.
- 9 Britt, J. P., F. Benaliouad, R. A. McDevitt, G. D. Stuber, R. A. Wise, and A. Bonci. 2012. "Synaptic and Behavioral Profile of Multiple
10 Glutamatergic Inputs to the Nucleus Accumbens." *Neuron* 76 (4):790-803. doi: 10.1016/j.neuron.2012.09.040.
- 11 Carlezon, W. A., Jr., and M. J. Thomas. 2009. "Biological substrates of reward and aversion: a nucleus accumbens activity
12 hypothesis." *Neuropharmacology* 56 Suppl 1:122-32. doi: 10.1016/j.neuropharm.2008.06.075.
- 13 Carlson, K. S., M. R. Dillione, and D. W. Wesson. 2014. "Odor- and state-dependent olfactory tubercle local field potential
14 dynamics in awake rats." *J Neurophysiol* 111 (10):2109-23. doi: 10.1152/jn.00829.2013.
- 15 Cohen, J. Y., S. Haesler, L. Vong, B. B. Lowell, and N. Uchida. 2012. "Neuron-type-specific signals for reward and punishment in
16 the ventral tegmental area." *Nature* 482 (7383):85-U109. doi: 10.1038/nature10754.
- 17 DiBenedictis, B. T., A. O. Olugbemi, M. J. Baum, and J. A. Cherry. 2015. "DREADD-Induced Silencing of the Medial Olfactory
18 Tubercle Disrupts the Preference of Female Mice for Opposite-Sex Chemosignals(1,2,3)." *eNeuro* 2 (5). doi:
19 10.1523/ENEURO.0078-15.2015.
- 20 Doty, R. L. 1986. "Odor-Guided Behavior in Mammals." *Experientia* 42 (3):257-271. doi: Doi 10.1007/Bf01942506.
- 21 FitzGerald, B. J., K. Richardson, and D. W. Wesson. 2014. "Olfactory tubercle stimulation alters odor preference behavior and
22 recruits forebrain reward and motivational centers." *Frontiers in Behavioral Neuroscience* 8. doi: Artn 81
23 10.3389/Fnbeh.2014.00081.
- 24 Flagel, S. B., J. J. Clark, T. E. Robinson, L. Mayo, A. Czuj, I. Willuhn, C. A. Akers, S. M. Clinton, P. E. M. Phillips, and H. Akil. 2011. "A
25 selective role for dopamine in stimulus-reward learning." *Nature* 469 (7328):53-U63. doi: 10.1038/nature09588.
- 26 Gadziola, M. A., K. A. Tylicki, D. L. Christian, and D. W. Wesson. 2015. "The Olfactory Tubercle Encodes Odor Valence in Behaving
27 Mice." *Journal of Neuroscience* 35 (11):4515-4527. doi: 10.1523/Jneurosci.4750-14.2015.
- 28 Gadziola, M. A., and D. W. Wesson. 2016. "The Neural Representation of Goal-Directed Actions and Outcomes in the Ventral
29 Striatum's Olfactory Tubercle." *Journal of Neuroscience* 36 (2):548-560. doi: 10.1523/Jneurosci.3328-15.2016.
- 30 Gerfen, C. R., and D. J. Surmeier. 2011. "Modulation of striatal projection systems by dopamine." *Annu Rev Neurosci* 34:441-66.
31 doi: 10.1146/annurev-neuro-061010-113641.
- 32 Gunaydin, L. A., L. Grosenick, J. C. Finkelstein, I. V. Kauvar, L. E. Fenno, A. Adhikari, S. Lammel, J. J. Mirzabekov, R. D. Airan, K. A.
33 Zalocusky, K. M. Tye, P. Anikeeva, R. C. Malenka, and K. Deisseroth. 2014. "Natural Neural Projection Dynamics
34 Underlying Social Behavior." *Cell* 157 (7):1535-1551. doi: 10.1016/j.cell.2014.05.017.
- 35 Herrera, D. G., and H. A. Robertson. 1996. "Activation of c-fos in the brain." *Progress in Neurobiology* 50 (2-3):83-107. doi: Doi
36 10.1016/S0301-0082(96)00021-4.
- 37 Hikida, T., K. Kimura, N. Wada, K. Funabiki, and S. Nakanishi. 2010. "Distinct roles of synaptic transmission in direct and indirect
38 striatal pathways to reward and aversive behavior." *Neuron* 66 (6):896-907. doi: 10.1016/j.neuron.2010.05.011.
- 39 Hu, H. 2016. "Reward and Aversion." *Annu Rev Neurosci* 39:297-324. doi: 10.1146/annurev-neuro-070815-014106.
- 40 Igarashi, K. M., N. Ieki, M. An, Y. Yamaguchi, S. Nagayama, K. Kobayakawa, R. Kobayakawa, M. Tanifuji, H. Sakano, W. R. Chen, and
41 K. Mori. 2012. "Parallel Mitral and Tufted Cell Pathways Route Distinct Odor Information to Different Targets in the
42 Olfactory Cortex." *Journal of Neuroscience* 32 (23):7970-7985. doi: 10.1523/Jneurosci.0154-12.2012.
- 43 Ikemoto, S. 2003. "Involvement of the olfactory tubercle in cocaine reward: Intracranial self-administration studies." *Journal of*
44 *Neuroscience* 23 (28):9305-9311.

- 1 Ikemoto, S. 2005. "The supramammillary nucleus mediates primary reinforcement via GABA(A) receptors."
2 *Neuropsychopharmacology* 30 (6):1088-1095. doi: 10.1038/sj.npp.1300660.
- 3 Ikemoto, S. 2007. "Dopamine reward circuitry: Two projection systems from the ventral midbrain to the nucleus
4 accumbens-olfactory tubercle complex." *Brain Research Reviews* 56 (1):27-78. doi: 10.1016/j.brainresrev.2007.05.004.
- 5 Ikemoto, S., B. S. Glazier, J. M. Murphy, and W. J. McBride. 1998. "Rats self-administer carbachol directly into the nucleus
6 accumbens." *Physiology & Behavior* 63 (5):811-814. doi: Doi 10.1016/S0031-9384(98)00007-9.
- 7 Keeler, J. F., D. O. Pretecell, and T. W. Robbins. 2014. "Functional implications of dopamine D1 vs. D2 receptors: A 'prepare and
8 select' model of the striatal direct vs. indirect pathways." *Neuroscience* 282:156-75. doi:
9 10.1016/j.neuroscience.2014.07.021.
- 10 Kim, C. K., S. J. Yang, N. Pichamoorthy, N. P. Young, I. Kauvar, J. H. Jennings, T. N. Lerner, A. Berndt, S. Y. Lee, C. Ramakrishnan, T. J.
11 Davidson, M. Inoue, H. Bito, and K. Deisseroth. 2016. "Simultaneous fast measurement of circuit dynamics at multiple
12 sites across the mammalian brain." *Nature Methods* 13 (4):325-328. doi: 10.1038/Nmeth.3770.
- 13 Kobayakawa, K., R. Kobayakawa, H. Matsumoto, Y. Oka, T. Imai, M. Ikawa, M. Okabe, T. Ikeda, S. Itohara, T. Kikusui, K. Mori, and H.
14 Sakano. 2007. "Innate versus learned odour processing in the mouse olfactory bulb." *Nature* 450 (7169):503-8. doi:
15 10.1038/nature06281.
- 16 Koob, G. F., and N. D. Volkow. 2010. "Neurocircuitry of Addiction." *Neuropsychopharmacology* 35 (1):217-238. doi:
17 10.1038/npp.2009.110.
- 18 Li, A. A., L. Gong, and F. Q. Xu. 2011. "Brain-state-independent neural representation of peripheral stimulation in rat olfactory
19 bulb." *Proceedings of the National Academy of Sciences of the United States of America* 108 (12):5087-5092. doi:
20 10.1073/pnas.1013814108.
- 21 Li, Y., W. Zhong, D. Wang, Q. Feng, Z. Liu, J. Zhou, C. Jia, F. Hu, J. Zeng, Q. Guo, L. Fu, and M. Luo. 2016. "Serotonin neurons in the
22 dorsal raphe nucleus encode reward signals." *Nat Commun* 7:10503. doi: 10.1038/ncomms10503.
- 23 Liu, Z. X., J. F. Zhou, Y. Li, F. Hu, Y. Lu, M. Ma, Q. R. Feng, J. E. Zhang, D. Q. Wang, J. W. Zeng, J. H. Bao, J. Y. Kim, Z. F. Chen, S. El
24 Mestikawy, and M. M. Luo. 2014. "Dorsal Raphe Neurons Signal Reward through 5-HT and Glutamate." *Neuron* 81
25 (6):1360-1374. doi: 10.1016/j.neuron.2014.02.010.
- 26 Mahon, S., J. M. Deniau, and S. Charpier. 2004. "Cortico-striatal plasticity: life after the depression." *Trends Neurosci* 27
27 (8):460-7. doi: 10.1016/j.tins.2004.06.010.
- 28 Millhouse, O. E., and L. Heimer. 1984. "Cell Configurations in the Olfactory Tubercle of the Rat." *Journal of Comparative*
29 *Neurology* 228 (4):571-597. doi: DOI 10.1002/cne.902280409.
- 30 Mooney, K. E., A. Inokuchi, J. B. Snow, Jr., and C. P. Kimmelman. 1987. "Projections from the ventral tegmental area to the
31 olfactory tubercle in the rat." *Otolaryngol Head Neck Surg* 96 (2):151-7.
- 32 Murata, K., M. Kanno, N. Ieki, K. Mori, and M. Yamaguchi. 2015. "Mapping of Learned Odor-Induced Motivated Behaviors in the
33 Mouse Olfactory Tubercle." *J Neurosci* 35 (29):10581-99. doi: 10.1523/JNEUROSCI.0073-15.2015.
- 34 Osakada, F., T. Mori, A. H. Cetin, J. H. Marshel, B. Virgen, and E. M. Callaway. 2011. "New rabies virus variants for monitoring and
35 manipulating activity and gene expression in defined neural circuits." *Neuron* 71 (4):617-31. doi:
36 10.1016/j.neuron.2011.07.005.
- 37 Rodd-Henricks, Z. A., D. L. McKinzie, T. K. Li, J. M. Murphy, and W. J. McBride. 2002. "Cocaine is self-administered into the shell
38 but not the core of the nucleus accumbens of Wistar rats." *Journal of Pharmacology and Experimental Therapeutics*
39 303 (3):1216-1226. doi: 10.1124/jpet.102.038950.
- 40 Roeper, J. 2013. "Dissecting the diversity of midbrain dopamine neurons." *Trends in Neurosciences* 36 (6):336-342. doi:
41 10.1016/j.tins.2013.03.003.
- 42 Scott, J. W., R. L. McBride, and S. P. Schneider. 1980. "The Organization of Projections from the Olfactory-Bulb to the Piriform
43 Cortex and Olfactory Tubercle in the Rat." *Journal of Comparative Neurology* 194 (3):519-534. doi: DOI
44 10.1002/cne.901940304.
- 45 Stamatakis, A. M., and G. D. Stuber. 2012. "Activation of lateral habenula inputs to the ventral midbrain promotes behavioral
46 avoidance." *Nature Neuroscience* 15 (8):1105-+. doi: 10.1038/nn.3145.

- 1 Steinberg, E. E., J. R. Boivin, B. T. Saunders, I. B. Witten, K. Deisseroth, and P. H. Janak. 2014. "Positive reinforcement mediated by
2 midbrain dopamine neurons requires D1 and D2 receptor activation in the nucleus accumbens." *PLoS One* 9
3 (4):e94771. doi: 10.1371/journal.pone.0094771.
- 4 Stoof, J. C., and J. W. Keabian. 1981. "Opposing roles for D-1 and D-2 dopamine receptors in efflux of cyclic AMP from rat
5 neostriatum." *Nature* 294 (5839):366-368. doi: 10.1038/294366a0.
- 6 Striano, B. M., D. J. Barker, A. P. Pawlak, D. H. Root, A. T. Fabbriatore, K. R. Coffey, J. P. Stamos, and M. O. West. 2014. "Olfactory
7 Tubercle Neurons Exhibit Slow-Phasic Firing Patterns During Cocaine Self-Administration." *Synapse* 68 (7):321-323. doi:
8 10.1002/syn.21744.
- 9 Tronel, S., and S. J. Sara. 2002. "Mapping of olfactory memory circuits: Region-specific c-fos activation after odor-reward
10 associative learning or after its retrieval." *Learning & Memory* 9 (3):105-111. doi: 10.1101/lm.47802.
- 11 Ungless, M. A., E. Argilli, and A. Bonci. 2010. "Effects of stress and aversion on dopamine neurons: Implications for addiction."
12 *Neuroscience and Biobehavioral Reviews* 35 (2):151-156. doi: 10.1016/j.neubiorev.2010.04.006.
- 13 Voorn, P., B. Jorritsmabyham, C. Vandijk, and R. M. Buijs. 1986. "The Dopaminergic Innervation of the Ventral Striatum in the Rat
14 - a Light-Microscopic and Electron-Microscopic Study with Antibodies against Dopamine." *Journal of Comparative*
15 *Neurology* 251 (1):84-99. doi: DOI 10.1002/cne.902510106.
- 16 Wei, P., N. Liu, Z. Zhang, X. Liu, Y. Tang, X. He, B. Wu, Z. Zhou, Y. Liu, J. Li, Y. Zhang, X. Zhou, L. Xu, L. Chen, G. Bi, X. Hu, F. Xu, and L.
17 Wang. 2015. "Processing of visually evoked innate fear by a non-canonical thalamic pathway." *Nat Commun* 6:6756.
18 doi:10.1038/ncomms7756.
- 19 Wesson, D. W., and D. A. Wilson. 2010. "Smelling sounds: olfactory-auditory sensory convergence in the olfactory tubercle." *J*
20 *Neurosci* 30 (8):3013-21. doi: 10.1523/JNEUROSCI.6003-09.2010.
- 21 Wesson, D. W., and D. A. Wilson. 2011. "Sniffing out the contributions of the olfactory tubercle to the sense of smell: Hedonics,
22 sensory integration, and more?" *Neuroscience and Biobehavioral Reviews* 35 (3):655-668. doi:
23 10.1016/j.neubiorev.2010.08.004.
- 24 Wickens, J. R., J. N. Reynolds, and B. I. Hyland. 2003. "Neural mechanisms of reward-related motor learning." *Curr Opin*
25 *Neurobiol* 13 (6):685-90.
- 26 Wieland, S., D. Du, M. J. Oswald, R. Parlato, G. Kohr, and W. Kelsch. 2014. "Phasic Dopaminergic Activity Exerts Fast Control of
27 Cholinergic Interneuron Firing via Sequential NMDA, D2, and D1 Receptor Activation." *Journal of Neuroscience* 34
28 (35):11549-11559. doi: 10.1523/Jneurosci.1175-14.2014.
- 29 Wilson, D. A., and R. M. Sullivan. 2011. "Cortical Processing of Odor Objects." *Neuron* 72 (4):506-519. doi:
30 10.1016/j.neuron.2011.10.027.
- 31 Worley, P. F., R. V. Bhat, J. M. Baraban, C. A. Erickson, B. L. Mcnaughton, and C. A. Barnes. 1993. "Thresholds for Synaptic
32 Activation of Transcription Factors in Hippocampus - Correlation with Long-Term Enhancement." *Journal of*
33 *Neuroscience* 13 (11):4776-4786.
- 34 Xiong, A., and D. W. Wesson. 2016. "Illustrated Review of the Ventral Striatum's Olfactory Tubercle." *Chemical Senses* 41
35 (7):549-555. doi: 10.1093/chemse/bjw069.
- 36 Yang, H., J. Yang, W. Xi, S. Hao, B. Luo, X. He, L. Zhu, H. Lou, Y. Q. Yu, F. Xu, S. Duan, and H. Wang. 2016. "Laterodorsal tegmentum
37 interneuron subtypes oppositely regulate olfactory cue-induced innate fear." *Nat Neurosci* 19 (2):283-9. doi:
38 10.1038/nn.4208.
- 39 Yang, Y., Z. H. Wang, S. Jin, D. Gao, N. Liu, S. P. Chen, S. Zhang, Q. Liu, E. Liu, X. Wang, X. Liang, P. Wei, X. Li, Y. Li, C. Yue, H. L. Li, Y. L.
40 Wang, Q. Wang, D. Ke, Q. Xie, F. Xu, L. Wang, and J. Z. Wang. 2016. "Opposite monosynaptic scaling of BLP-vCA1 inputs
41 governs hopefulness- and helplessness-modulated spatial learning and memory." *Nat Commun* 7:11935. doi:
42 10.1038/ncomms11935.
- 43 Yawata, S., T. Yamaguchi, T. Danjo, T. Hikida, and S. Nakanishi. 2012. "Pathway-specific control of reward learning and its flexibility
44 via selective dopamine receptors in the nucleus accumbens." *Proc Natl Acad Sci U S A* 109 (31):12764-9. doi:
45 10.1073/pnas.1210797109.
- 46 Zhang, Z. J., H. R. Zhang, P. J. Wen, X. T. Zhu, L. Wang, Q. Liu, J. Wang, X. B. He, H. D. Wang, and F. Q. Xu. 2017. "Whole-Brain

1 Mapping of the Inputs and Outputs of the Medial Part of the Olfactory Tubercle." *Frontiers in Neural Circuits* 11. doi:
2 ARTN5210.3389/fncir.2017.00052.
3

1 Figure legends

2 Figure 1. Inputs of the mOT. (A) Schematic for the tracing experiment. RV-dG-GFP was unilaterally injected into the mOT of C57BL/6 mice.
3 The representative coronal brain section showed the injection site in the mOT. (B) Magnification of RV-dG-GFP labeled neurons in the mOT.
4 (C-G) GFP positive cells were widely distributed in the OB (C-E), PCX (F) and VTA (G) with RV retrograde tracing. In the OB, the labeled cells
5 were mainly distributed in the mitral cell layers (D), while also sparsely located in the external plexiform layer (E, red circles). (H, I) TH was
6 co-stained with RV-dG-GFP labeled neurons in the VTA, followed by mOT injection of RV-dG-GFP. (J) Statistical chart showed that more than
7 half of the GFP+ neurons co-express TH (n = 3). Nuclei of all the slices were stained blue with DAPI. Scale bar: 200 μ m.

8
9 Figure 2. Reward increased Ca^{2+} signals of VTA-mOT DAergic projection. (A) Schematic of the fiber photometry setup for recording of the
10 VTA-mOT DAergic projection from DAT-Cre mice. (B) Raw traces of GCaMP and control GFP fluorescence as the mice lick sucrose solution.
11 $\Delta F/F$ represents change in fluorescence from the mean level before task. (C) The heatmap illustrated Ca^{2+} signal responses of 8 sucrose licking
12 bouts from a representative mouse. Color bar: $\Delta F/F$. (D) Responses to sucrose solution (left), food pellets (middle) and social interaction (right)
13 for the control and GCaMP6m-expressing mice. *P < 0.05.

14
15 Figure 3. Activation of the VTA-mOT DAergic projection produced acute place preference. (A) Schematic for virus injection to manipulate the
16 VTA-mOT DAergic projections. AAV9-EF1a-floxed-ChR2-mCherry or the AAV9-EF1a-floxed-mCherry was unilaterally injected into the
17 VTA of DAT-Cre mice. (B) ChR2-mCherry positive axons were densely distributed in the mOT. (C, D) Co-localization of the TH with
18 ChR2-mCherry in the VTA neurons. (E) Statistical chart showed that ChR2-mCherry was relatively restricted to TH positive neurons (n = 3). (F)
19 Blue light stimulation of the VTA-mOT DAergic projections increased the c-fos expression levels in the OT, NAc, and PCX, while the c-fos
20 expression levels in the LSX and dSTR had no significant changes (n.s., P > 0.05). (G, H) Optical fibers were implanted in the mOT of control
21 or ChR2-expressing mice. (I, J) Representative real-time place preference (RTPP) tracks illustrated light-evoked behavioral preference in
22 ChR2-expressing mice (right, n = 7), but not in control mice (left, n = 7). (K) ChR2-expressing mice showed a significant preference for light
23 stimulation chamber compared with control mice in the RTPP test. *P < 0.05, ** P < 0.01, *** P < 0.001. Scale bar: 200 μ m.

24
25 Figure 4. Activation of the VTA-mOT DAergic projection produced positive reinforcement. (A) Schematics for iClass training. Mice explored in
26 an open field containing a rectangle in the center, which is marked red and 1/10 of the total area, for five consecutive days. In the first day (Pre)
27 and last day (Test) mice received no light stimulation. During the three consecutive training days (L1, L2, L3), light pulses (483 nm) at 20 Hz
28 were delivered to activate the VTA-mOT DAergic projection when mice were in the rectangle (bottom), and terminated until they left the
29 rectangle (Top). (B-D) ChR2-mCherry-expressing mice (n = 7) increased entry times (B) and retention (C, D) for central area when compared
30 with control mice (n = 7). The dashed line represents the percentage of the marked rectangle to the total. *P < 0.05, ** P < 0.01, *** P < 0.001.
31 The preference was turned up at the first training day, increased with the training sections, and maintained to the test day (B, C). Learning curves
32 showed that mice took 3-6 min to overcome their instinctive avoidance for the central area in the first training day (D). The center preference
33 increased with training time and days. (E, F) Representative iClass tracks illustrated light-evoked center preference in ChR2-expressing mice
34 (bottom, F) but not in the control mice (top, E).

1

2 Figure 5. Activation of the VTA (DAergic)-mOT pathway elicited or altered odor-preference. (A) The time-course for optogenetic activation of
 3 the VTA (DAergic)-mOT pathway paired with odor stimulations and test for odor-preference. (B) Schematic for the odor-light pairing training.
 4 (C) For a pair of neutral odors which are equivalently sampled by the naive mice, the percentage of investigation time for the paired odor,
 5 geraniol, was significantly higher than the non-paired one, carvone after pairing with activation of this pathway (*P < 0.05, n = 8). (D) For an
 6 odor pair with one that is preferred and one that is aversive to the naive mice, the percentage of investigation time was significantly increased for
 7 the aversive odor, TMT, equivalent to the previous preferred odor, sesame butter after pairing with activation of this pathway (*P < 0.05, n = 8).
 8 (E) Schematic for pre-treatment of the D1R and D2R antagonist (SCH-23390 and raclopride) before optogenetic activation of the VTA
 9 (DAergic)-mOT pathway paired with odor stimulation. (F) The percentage of investigation time for the paired odor, geraniol, was not
 10 significantly changed followed by the antagonist administration (P=0.757, n = 6). However, the mice that pretreated with normal saline still
 11 showed significant preference to the paired odor (*P < 0.05, n=6).

12

13 Figure 6. VTA DAergic neurons segregatedly innervate the NAc and the mOT. (A) Schematic for labeling the mOT and NAc co-innervated VTA
 14 neurons by dual RV labeling. (B) RV-dG-DsRed and RV-dG-GFP was injected into the mOT and NAc, respectively. (C) The VTA neurons were
 15 labeled by both RV-dG-DsRed and RV-dG-GFP. (D) The magnification of VTA labeled neurons in C. (E) The co-labeled rate (1.65%) of the
 16 VTA neurons by both GFP and dsRed were negligible, which implied that it may not be common for a VTA DAergic neuron to co-innervate the
 17 NAc and the mOT. Scale bar: 200 μm.

18

19 Figure 7. Inactivation of the mOT-projecting VTA DAergic neurons decreased the odor-cue based reward learning and learnt odor-preference.
 20 (A) The schematic for specifically targeting the mOT-projecting VTA DAergic neurons by injecting CAV-CMV-Cre and
 21 AAV-EF1a-floxed-hM4Di-mCherry/AAV-EF1a-floxed-mCherry into the mOT and VTA, respectively. (B, C) The mCherry-labeled neurons in
 22 the VTA in control and hM4Di-expressing mice. (D) The projections from the VTA mCherry-labeled neurons to the OT were mainly found in
 23 the medial part of the OT. (E, F) Most of the mCherry-labeled neurons in the VTA were also co-expressing TH (90.86 %). (G) After the
 24 odor-preference was established (left bar pair), inhibition of the mOT-projecting VTA DAergic neurons abolished the paired preference
 25 (P=0.214, n = 5 for mCherry and 6 for hM4Di group, respectively). (H) Inactivation of this pathway in well-trained mice (left bar pair) didn't
 26 influence the learnt Go-no go task performance (middle bar pair; Control group, P=0.373; hM4Di group, P=0.312), but significantly decreased
 27 the performance in learning a new pair of odors with the same paradigm (right bar pair; P<0.01, n = 5 for mCherry and 6 for hM4Di group,
 28 respectively).

29

30 Figure 8. Optogenetic inactivation of VTA-mOT DAergic projections during odor-food associative learning abolished the establishment of S+
 31 odor preference. (A) The schematic for viral injection and optic fiber implants. (B) eNpHR3.0-mCherry was densely expressed in the VTA
 32 neurons. (C) Representative coronal sections showed terminal expression of eNpHR3.0-mCherry and optic fiber implants in the bilateral mOT.
 33 The borders for the mOT and lateral OT were indicated by dark green triangles. Scale bar: 100 μm. (D) The S+ odor preference can't be
 34 established after odor-food associative learning by simultaneously light inhibition of the mOT DAergic projections from the VTA (each group n

1 = 6). Scale bar: 100 μ m.

2

3 Figure supplement legends

4 Figure 2-figure supplement 1. The VTA-mOT DAergic projection showed a higher response to sucrose reward than the bitter quinine solution.

5 (A) Raw fibre photometry recorded signals of VTA-mOT DAergic projection in response to sucrose or quinine solution stimuli. (B) Bitter
6 quinine solution elicited weaker response than the reward one (sucrose) in DAT-Cre mice by using fibre photometry ($1.68\% \pm 0.19\%$ for sucrose
7 solution; $0.74\% \pm 0.04\%$ for quinine solution, $P < 0.001$, $n = 5$).

8 Figure 2-figure supplement 2. The mOT neurons are activated by different odor stimulations. (A) Schematic of the fibre photometry recording
9 from the mOT neurons. (B) Representative traces of GCaMP fluorescence in response to odor and mineral oil stimulations for the
10 GCaMP6m-expressing C57BL/6 mice.

11 Figure 3-figure supplement 1. Optogenetic activation of the VTA-mOT DAergic projections. (A) AAV9-EF1a-floxed-ChR2-mCherry was
12 injected into the VTA of DAT-Cre or C57BL/6 mice. The mCherry was densely expressed in VTA neurons (bottom), but was negatively found
13 in the VTA of C57BL/6 mice (top). (B) Blue light stimulation at 20 Hz reliably induced action potentials in ChR2-expressing neurons. (C)
14 Representative coronal sections showed the c-fos expression in the OT in control (top) and the ChR2-mCherry-expressing mice (bottom). The
15 yellow boxes represented the location of the optic fiber in the mOT. (D) Representative c-fos expression patterns in the dSTR, LSX, NAc and
16 PCX in the control (top) and the ChR2-mCherry-expressing mice (bottom). Scale bar: 200 μ m.

17 Figure 7-figure supplement 1. Only a small portion of the VTA DAergic neurons were labeled by CAV-CMV-Cre. (A) The representative coronal
18 brain section showed the TH and mCherry co-expression in the VTA neurons after CAV-CMV-Cre and AAV9-EF1a-floxed-mCherry injected
19 into the mOT and VTA respectively, (B) The mCherry-positive cells only account for a small portion (37.20 %) of the whole population of VTA
20 DAergic neurons. Scale bar: 200 μ m.

21

22 Video legends

23 Video 1. Pre-phase (pre) of iClass task of a ChR2 expressing mouse. The fiber patch cord was connected but no light was delivered.

24

25 Video 2. The first light-training session (L1) of iClass task of the ChR2 expressing mouse. When the central of the animal was located within the
26 marked central rectangular area, 10 mW blue light pulses at 20 Hz were constantly delivered into the mOT.

27

28 Video 3. The second light-training session (L2) of iClass task of the ChR2 expressing mouse. When the central of the animal was located within
29 the marked central rectangular area, 10 mW blue light pulses at 20 Hz were constantly delivered into the mOT.

30

31 Video 4. The third light-training session (L3) of iClass task of the ChR2 expressing mouse. When the central of the animal was located within
32 the marked central rectangular area, 10 mW blue light pulses at 20 Hz were constantly delivered into the mOT.

33

34 Video 5. The test day (test) of iClass task of the ChR2 expressing mouse. The fiber patch cord was connected but no light was delivered.

1
2
3

Video 6. Odor-preference test after odor-light pairing of a ChR2 expressing mouse.

4 Source data file information

5 Figure 1-Source Data 1: statistical result of RV infected neurons in the VTA that co-stained with tyrosine hydroxylase (TH).

6 Figure 2-Source Data 1: fiber photometry recording $\Delta F/F$ value to sucrose solution, food pellets and social interaction for the control and

7 GCaMP6m-expressing mice.

8 Figure 3-Source Data 1: statistical result of c-fos positive cells in the OT, NAc, LSX, dSTR and PCX after blue light stimulation of the VTA-mOT

9 DAergic projections.

10 Figure 3-Source Data 2: statistical result of the time percentage spent in the stimulated side in RTPP for the control and ChR2-expressing mice.

11 Figure 4-Source Data 1: statistical result of center entries and percentage of center duration in iClass training for the control and ChR2-expressing mice.

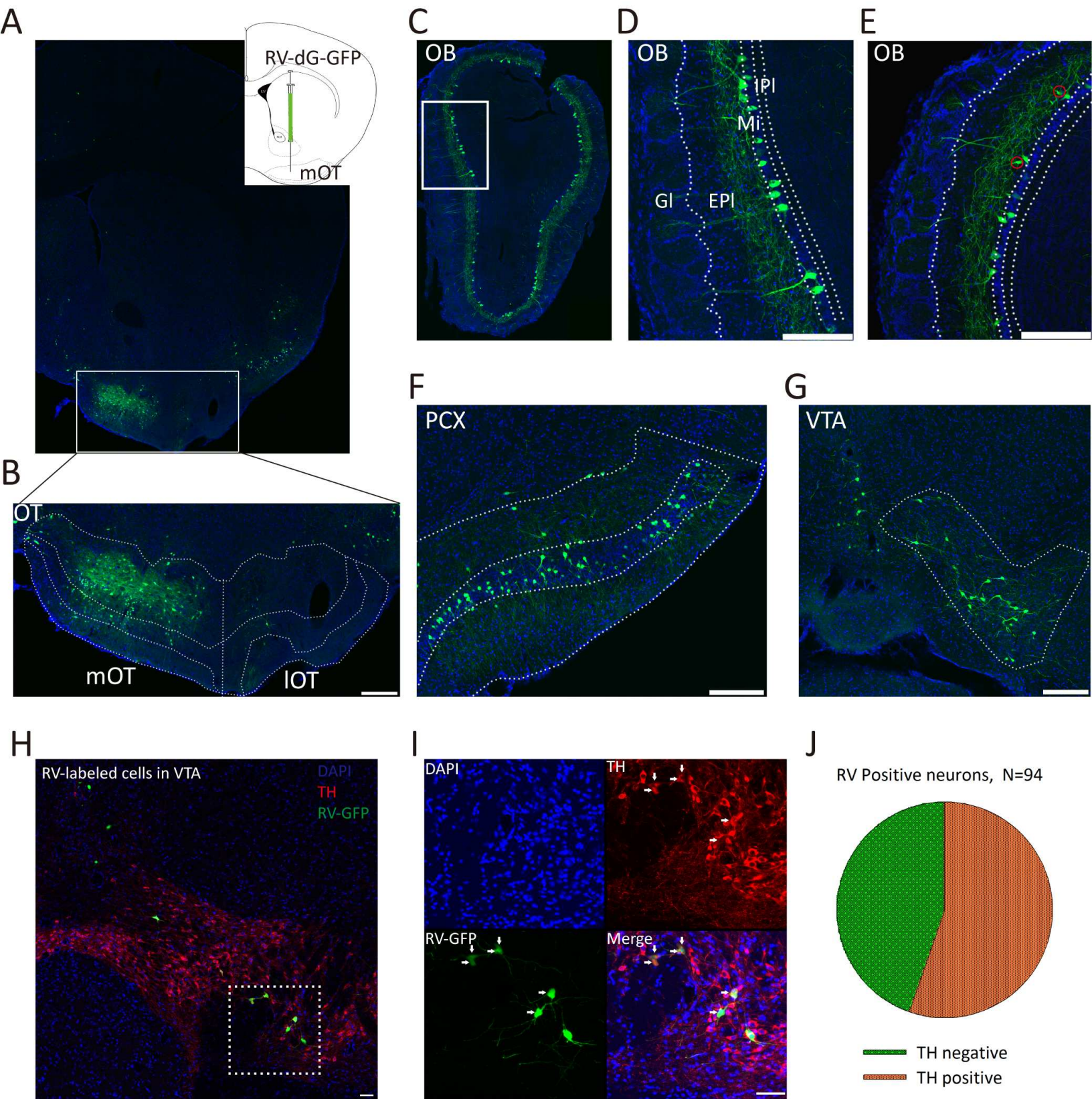
12 Figure 5-Source Data 1: statistical result of percentage of investigation time for TMT after odor-light pairing for the ChR2-expressing mice and

13 percentage of investigation time for geraniol after D1 and D2 dopamine receptor antagonist administration in the mOT.

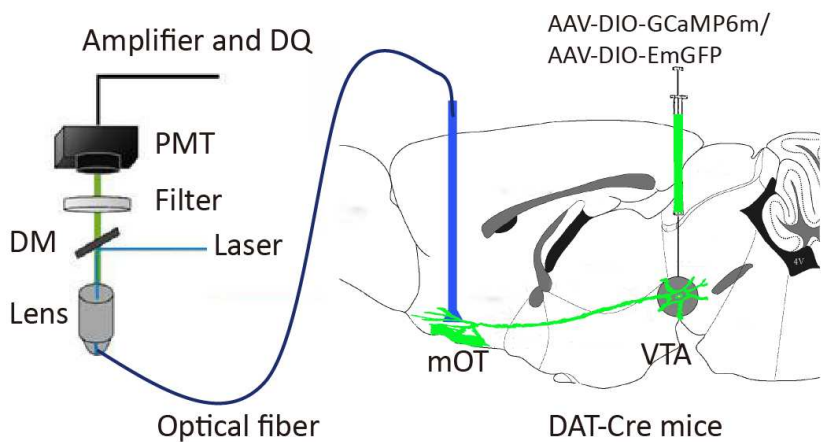
14 Figure 7-Source Data 1: statistical result of odor-preference test after inhibition of the mOT-projecting VTA DAergic neurons, accuracy of Go-no go

15 learning for hm4Di and control groups in well-trained mice.

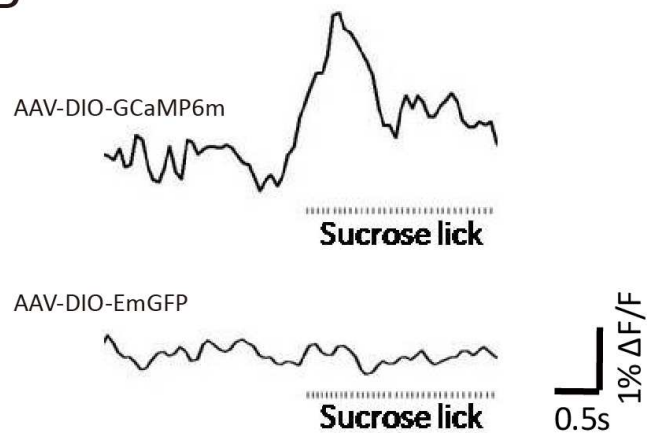
16 Figure 8-Source Data 1: statistical result of the odor-preference test after light inhibition of the mOT DAergic projections from the VTA.



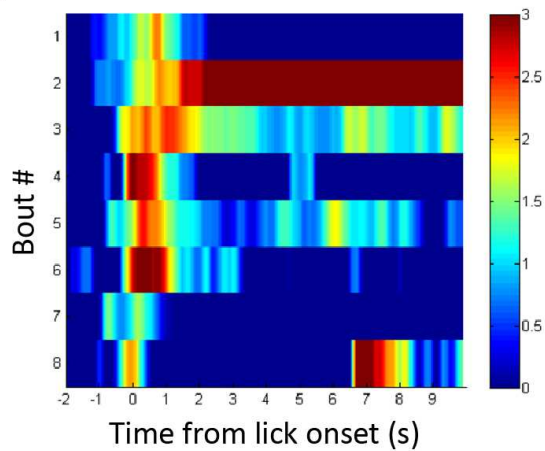
A



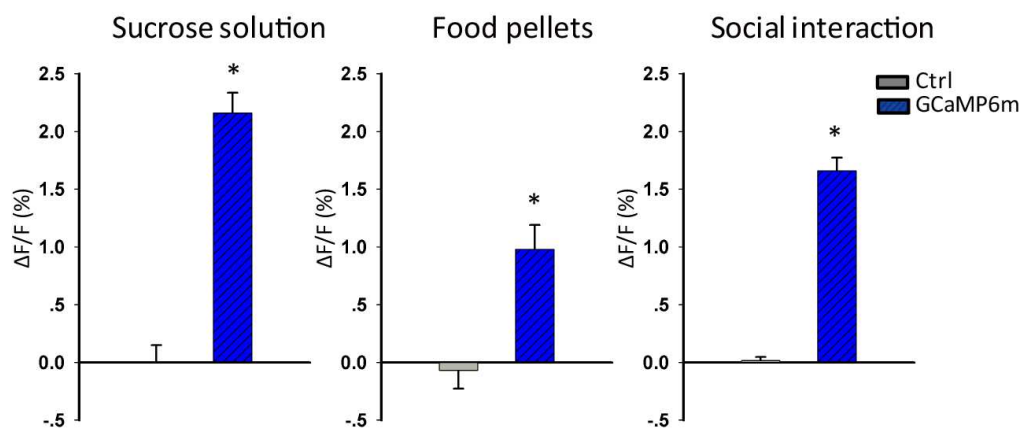
B



C



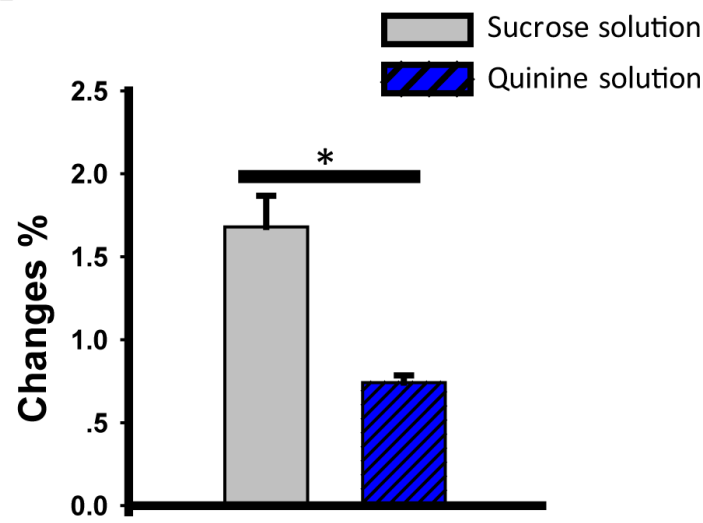
D



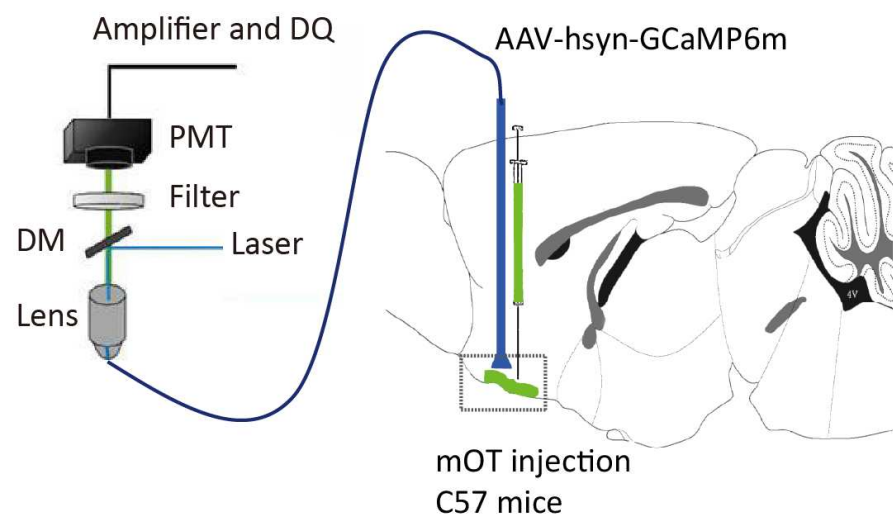
A



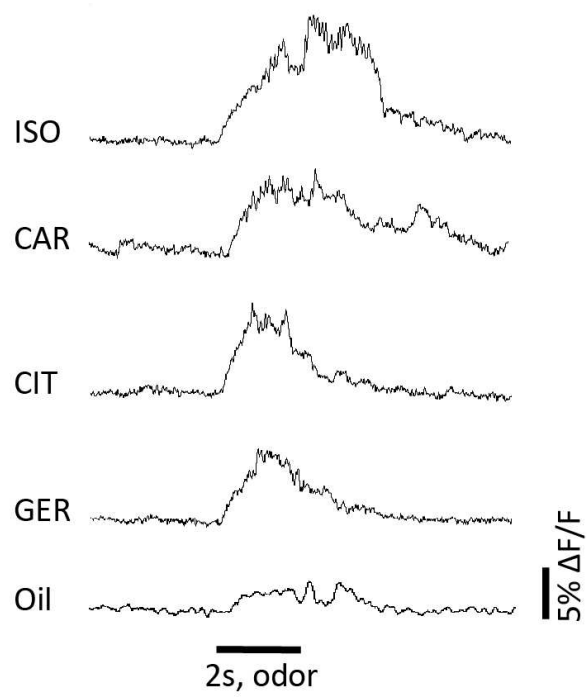
B

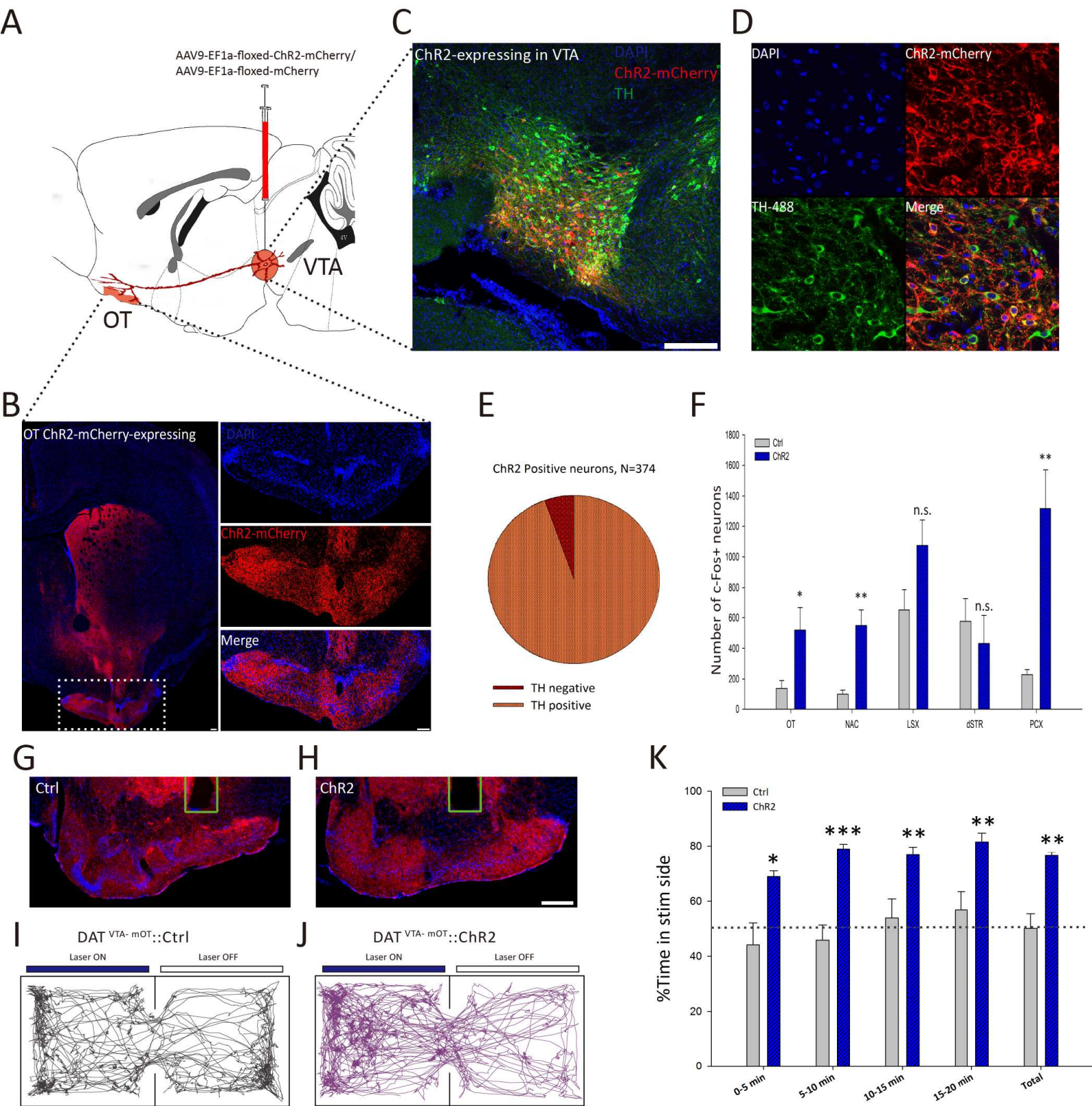


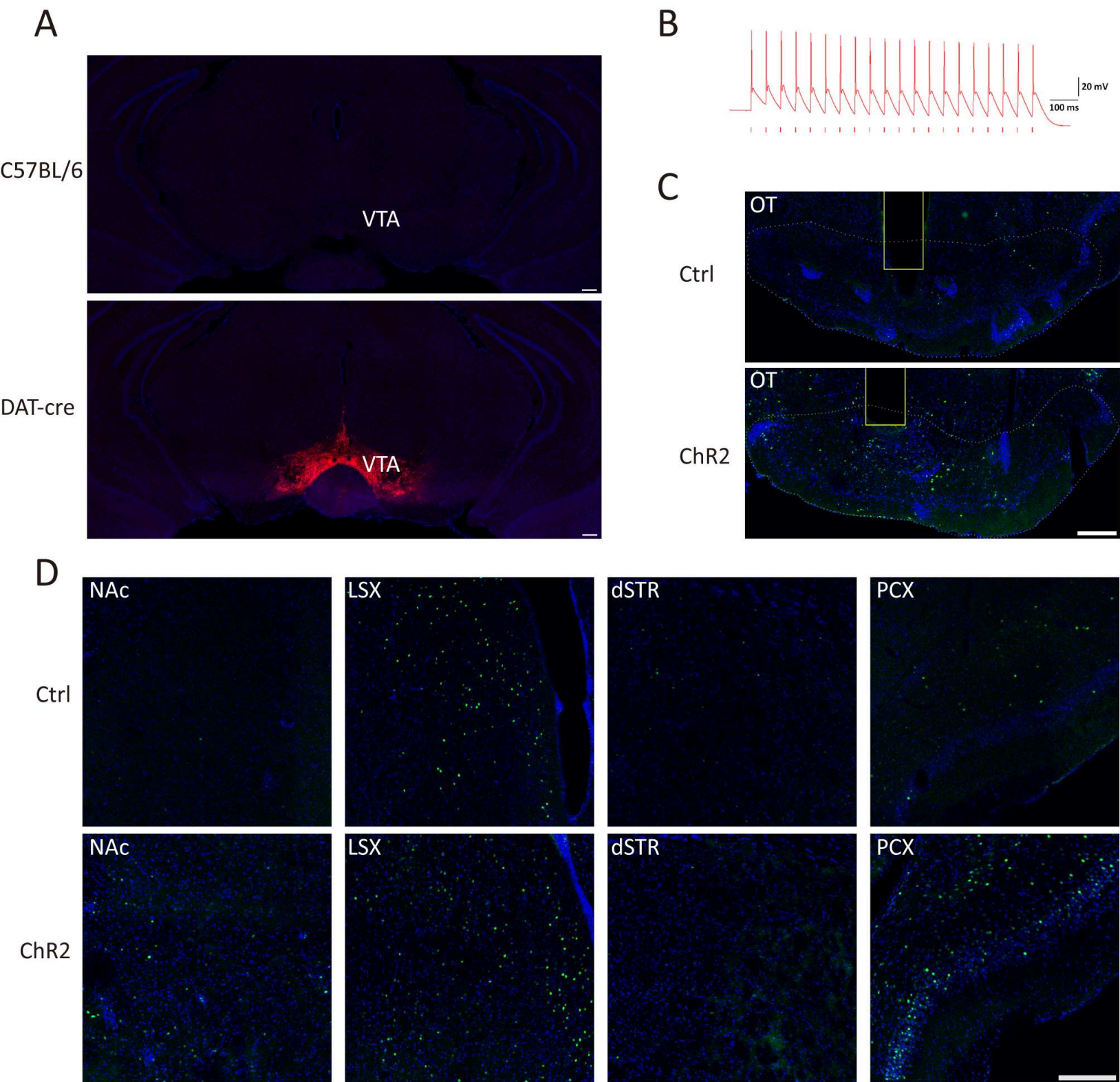
A



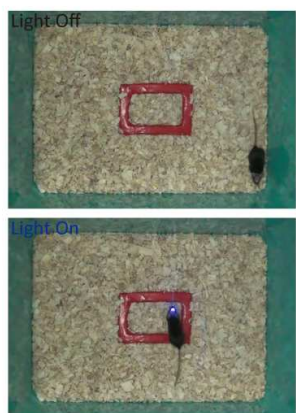
B



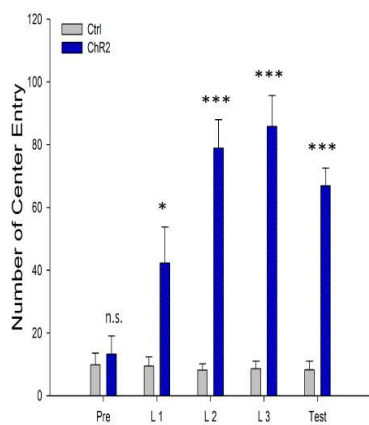




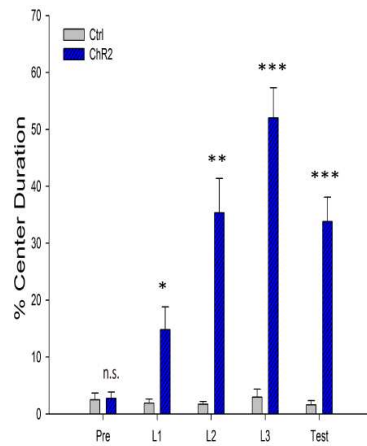
A



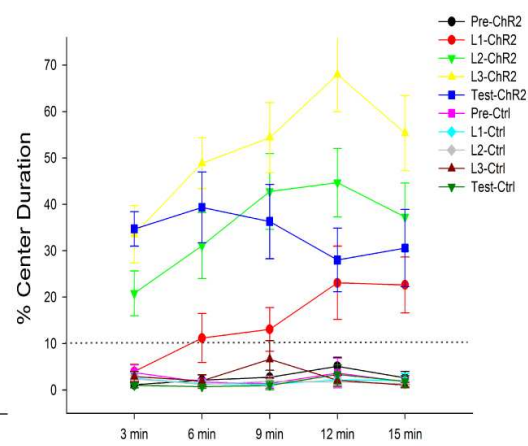
B



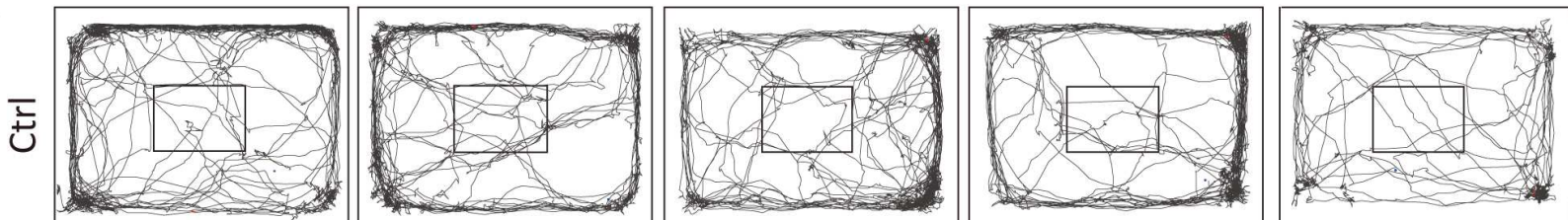
C



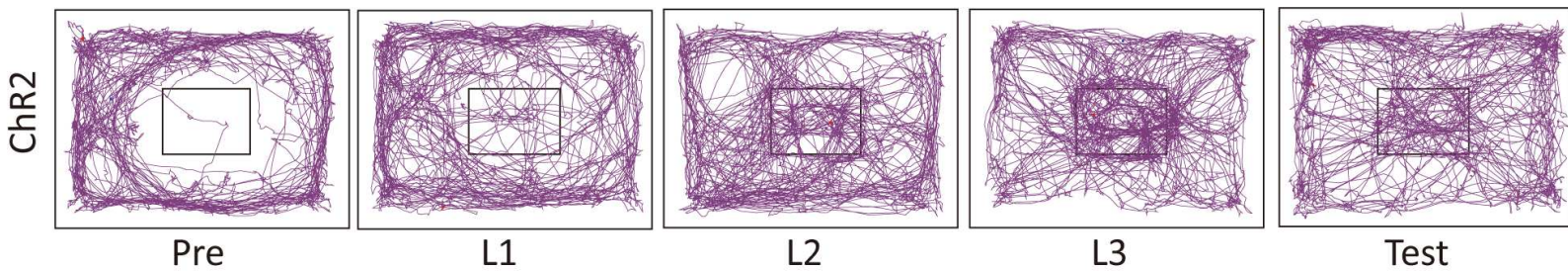
D



E



F



Pre

L1

L2

L3

Test

A

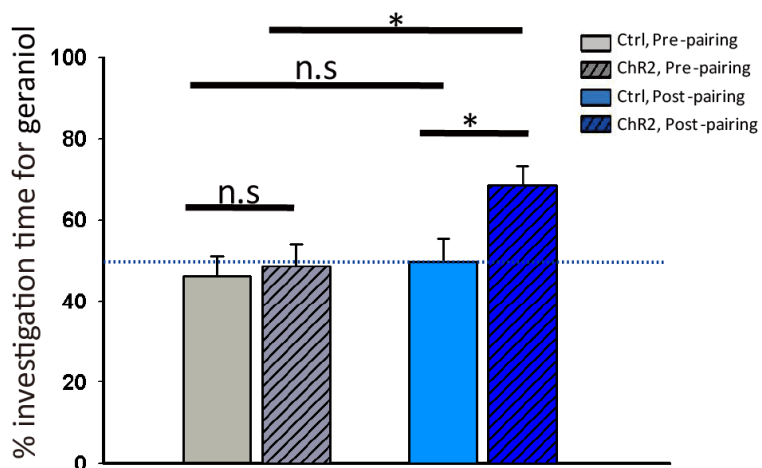


B

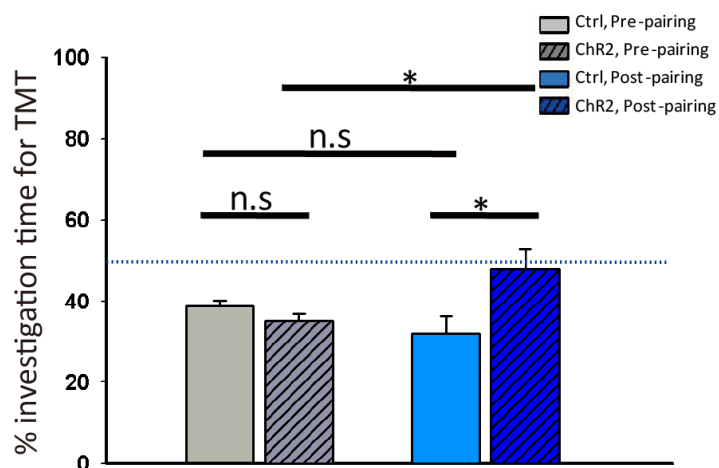


Odor A vs. Odor B:
 1. Geraniol vs. Carvone
 2. TMT vs. Sesame paste

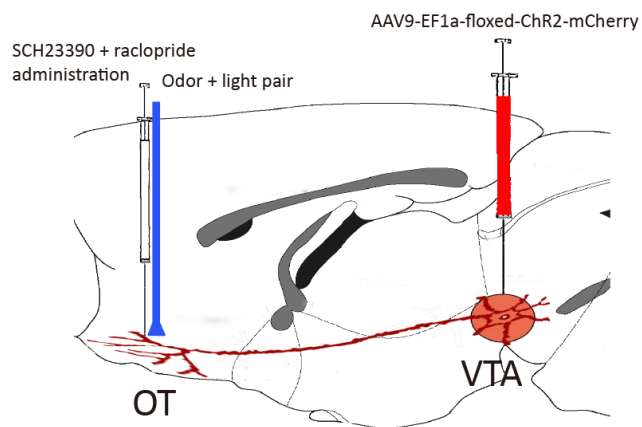
C



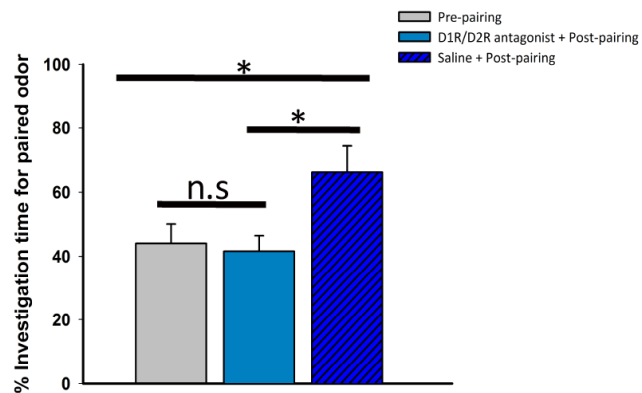
D

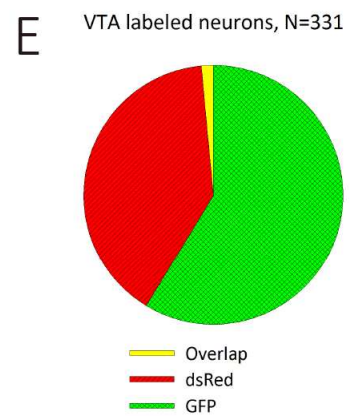
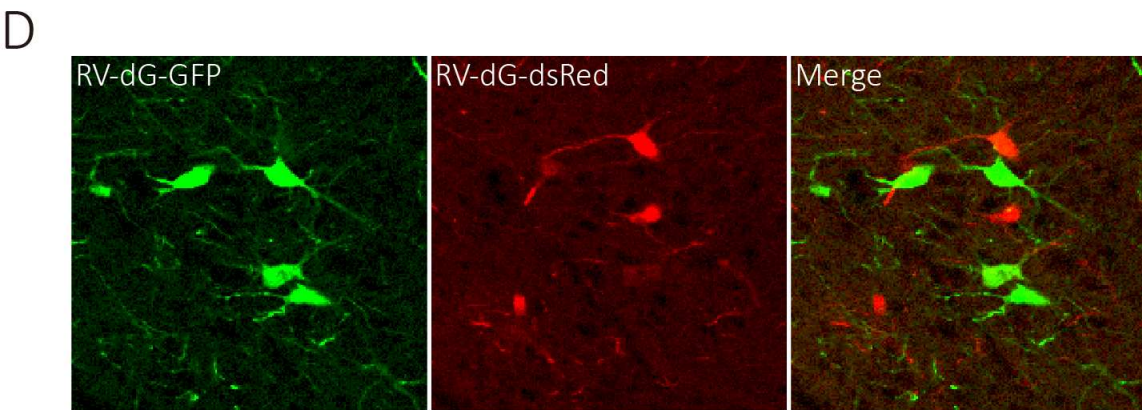
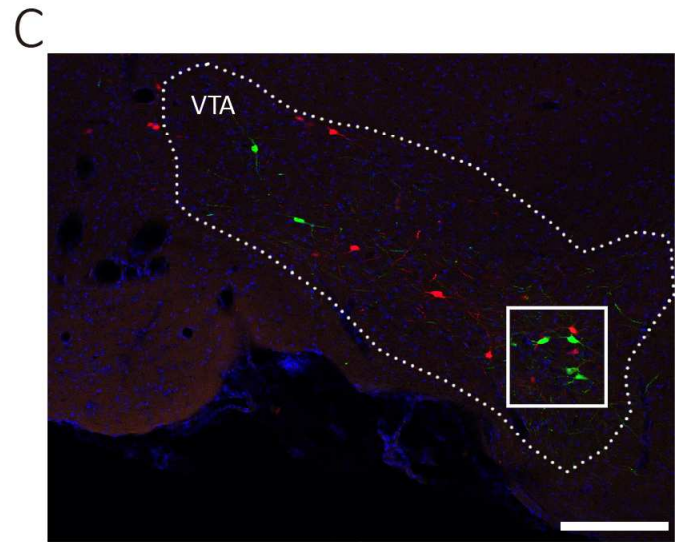
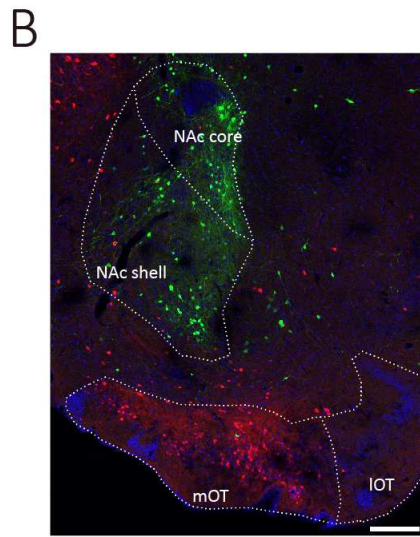
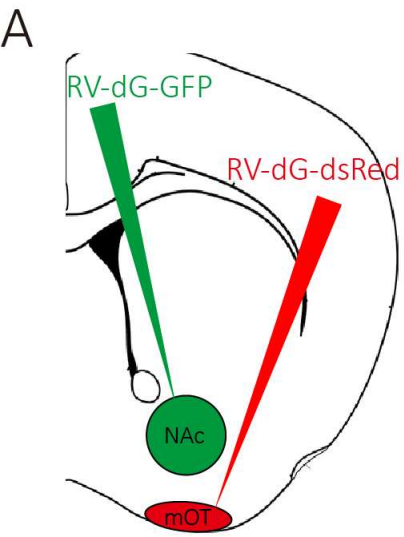


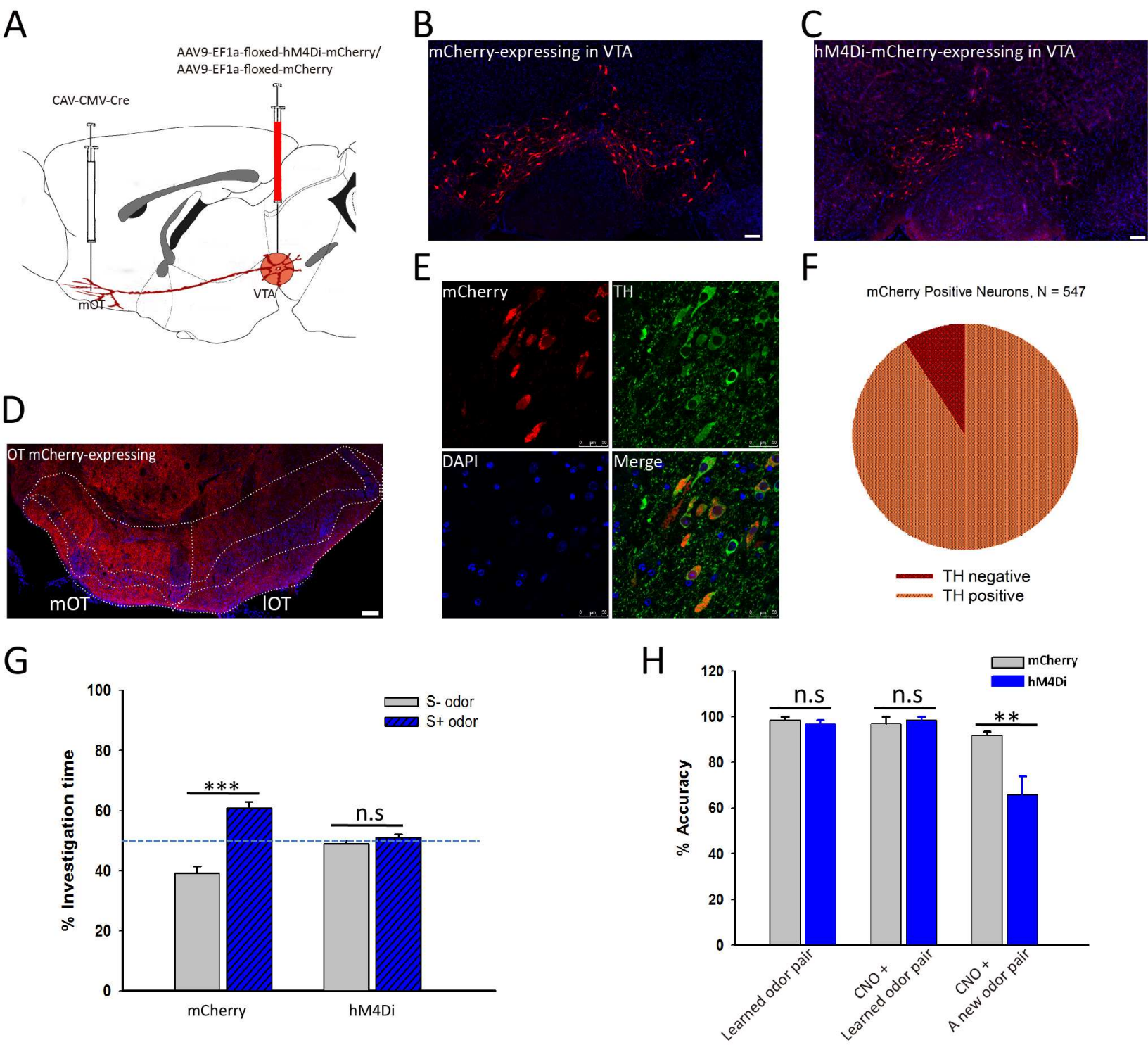
E



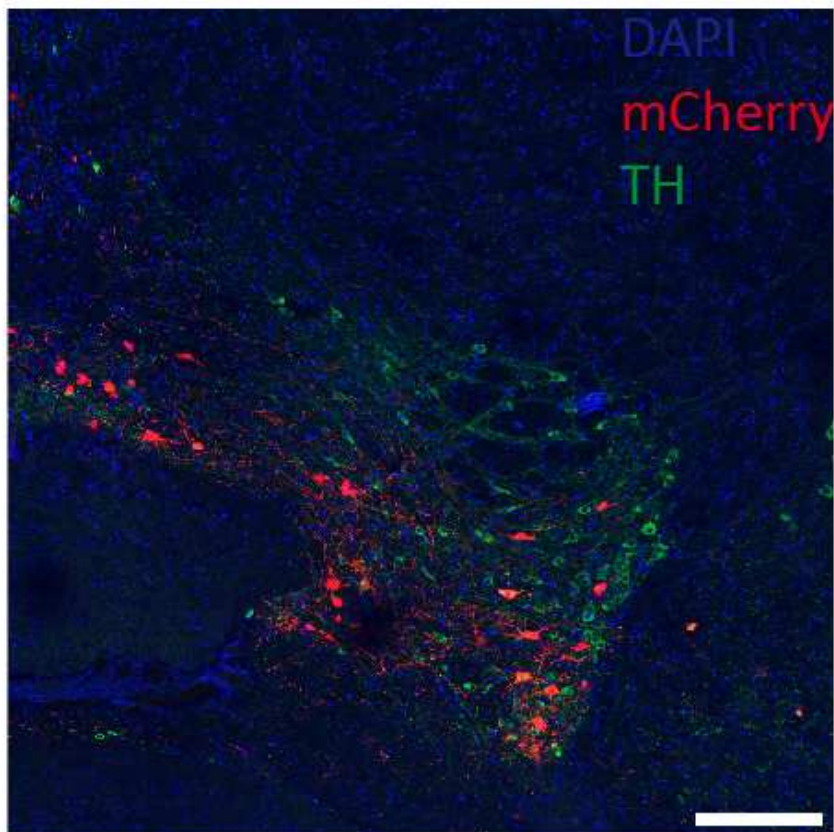
F





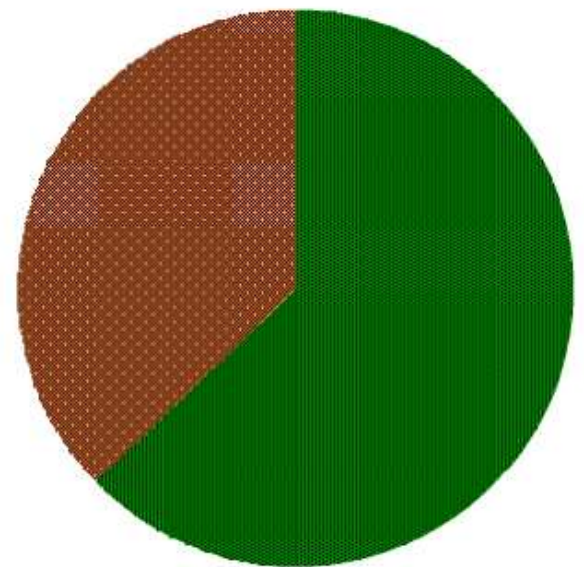


A



B

DAergic Neurons in the VTA, N = 1051

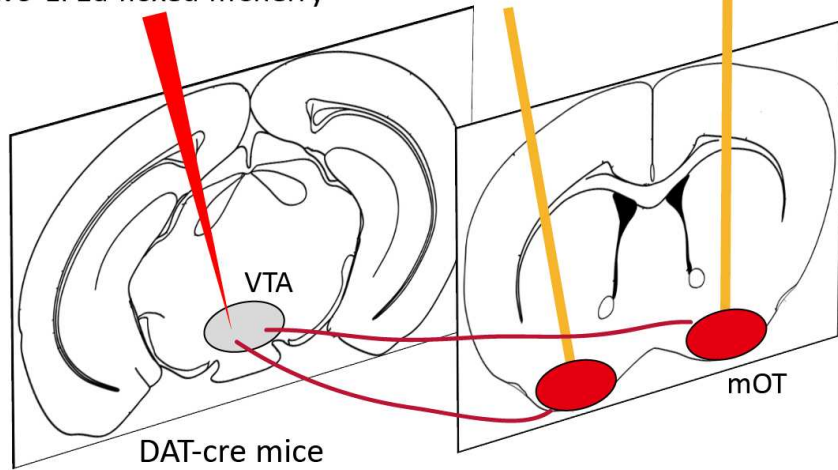


— mCherry positive
— mCherry negative

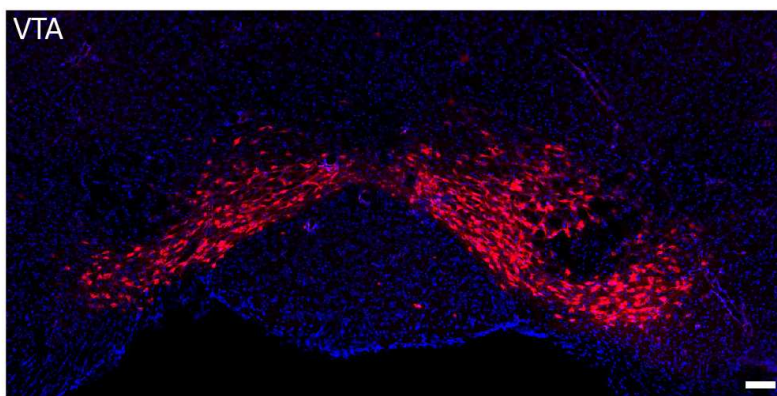
A

AAV9-EF1a-floxed-eNpHR3.0-mCherry/
AAV9-EF1a-floxed-mCherry

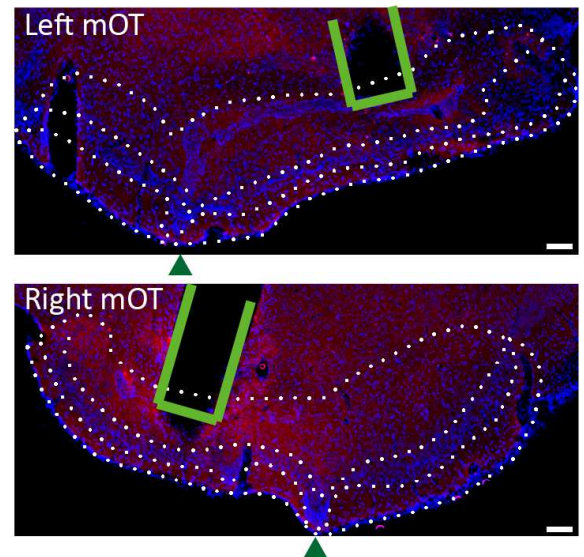
Optical fibers



B



C



D

